Table 1 Clinical findings and MDSCs

Clinical characteristics	MDSC ratio ≥22 ($n = 39$)	MDSC ratio <22 ($n = 84$)	p value
Age (year)	68.5	70.1	0.646
Sex (M/F)	29/10	54/30	0.267
AST (IU/l)	62.0	61.5	0.543
ALT (IU/l)	47.1	53.9	0.759
LDH (IU/l)	225	218	0.832
γGTP (IU/l)	78.0	76.0	0.252
Platelet (10^4/μl)	10.9	10.6	0.884
Prothrombin time (%)	75.2	82.3	0.045
Serum albumin (g/dl)	3.53	3.68	0.120
Total bilirubin (mg/dl)	1.21	0.94	0.286
WBC (/μl)	3910	3610	0.235
Neutrophil (%)	63.2	59.4	0.093
Lymphocyte (%)	26.1	29.5	0.047
Total cholesterol (mg/dl)	151	149	0.926
HbA1c (%)	5.27	5.43	0.197
Type IV collagen 7S (ng/ml)	8.2	7.3	0.086
DCP (mAU/ml)	5157	432	0.561
AFP (ng/ml)	1301	934	0.240
Tumor size (mm)	28.3	24.4	0.014
Tumor multiplicity (multiple/solitary)	27/12	42/42	0.046
TNM stage (I plus II/III plus IV)	17/22	60/24	0.003
Child-Pugh (A/B/C)	20/17/2	64/16/4	0.015
Etiology (HCV/HBV/others)	21/11/7	61/11/12	0.081
$CD4^+$ $CD25^+$ $CD127^{-/low}$ Tregs/ $CD4^+$ cells (%)	7.04	6.70	0.281

AST aspirate aminotransferase, *ALT* alanine aminotransferase, *LDH* lactic dehydrogenase, *γGTP* gamma glutamyltransferase, *WBC* white blood cell, *Hb* hemoglobin, *DCP* des-gamma-prothrombin, *AFP* alpha-fetoprotein, *HCV* hepatitis C virus, *HBV* hepatitis B virus, *Tregs* regulatory T cells

Chi-squared test with Yates' correction, unpaired t test, Mann–Whitney U test, and Kruskal–Wallis test were used for univariate analysis of two groups that were classified according to the frequency of MDSCs

multiplicity ($p = 0.010$) were significantly associated with HCC recurrence (Table 3). In multivariable analysis for recurrence, considering the variables in the univariate analysis with $p < 0.1$, only post-treatment MDSC ratio ≥22 % (HR 3.906, $p = 0.014$) was extracted as a significant risk factor for recurrence.

Discussion

MDSCs are expanded in pathological conditions such as malignancy, infection, or trauma and consist of a heterogeneous population of immature myeloid cells [15, 25]. In pathological conditions, immature myeloid cells are blocked to differentiate into mature macrophages, dendritic cells, or granulocytes; as a result, MDSCs are accumulated [15, 25]. MDSCs strongly inhibit anti-tumor immune response through a number of mechanisms [15, 25]. As monocytic subsets of MDSCs, $CD14^+HLA\text{-}DR^{-/low}$ MDSCs have been reported in various malignancies, including melanoma, multiple myeloma, prostate cancer, and bladder cancer [18, 20, 22, 35]. In the most recent study, Hoechst et al. [24] reported that $CD14^+HLA\text{-}DR^{-/low}$ MDSCs were significantly increased in HCC patients and they suppressed T cell functions through the induction of $CD4^+CD25^+Foxp3^+$ Treg.

In the present study, in addition to an increase in the number of MDSCs in HCC patients, we observed that the frequency was correlated with the progression of HCC. Consistent with our results, it has also been reported that the frequency of $CD14^+HLA\text{-}DR^{-/low}$ MDSCs was correlated with tumor progression in patients with other cancers, such as melanoma, prostate cancer, and bladder cancer [22, 35, 36]. However, the mechanisms behind the increase in MDSCs in advanced cancer patients are still unclear. As is well known, there is a close relationship between hepatocarcinogenesis and histological status of underlying liver [37, 38]. Therefore, the advance of hepatic fibrosis and the increase in inflammatory cell infiltration into liver might result in an increase in MDSCs following the progression of HCC. However, there was no relationship between the frequency of $CD14^+HLA\text{-}DR^{-/low}$ MDSCs and underlying liver status in our study. From our observations, increase in MDSCs was only correlated with tumor progression, but not with hepatic fibrosis or disease activity of CLD. This finding suggests that the expansion of $CD14^+HLA\text{-}DR^{-/low}$ MDSCs was mostly derived from the tumor environment itself, but not from inflammation or fibrosis of liver tissue around the tumor. The finding that a significant decrease in the frequency of circulating $CD14^+HLA\text{-}DR^{-/low}$ MDSCs is observed in most patients with curative treatment in this study supports this hypothesis. On the other hand, Tregs were also increased in HCC patients and associated with the progression of HCC. Though it was reported that MDSCs suppressed T cell function through the induction of Tregs, there was not a strong correlation between the frequencies of these two immunosuppressive cells.

Regarding the mechanism of MDSC expansion, we also analyzed the relationship between the serum cytokine levels and the frequency of MDSCs. We observed that the serum concentrations of IL-10, IL-13, and VEGF were significantly increased in the group with high frequency of MDSCs and there was a positive correlation between these cytokine levels and the frequency of MDSCs. Moreover, although there was no significant difference, the serum

Table 2 Serum cytokines and MDSCs

Cytokine	Healthy donor (mean) ($n = 13$)	MDSC ratio ≥ 22 (mean) ($n = 21$)	Range	MDSC ratio < 22 (mean) ($n = 31$)	Range	p value
IL-1ra	34.2	97.0	(21.5–600)	40.3	(3.4–151)	0.057
IL-2	10.5	38.1	(4.3–54.3)	11.3	(0.9–49.7)	0.055
IL-4	2.6	5.75	(1.47–11.9)	5.03	(0.71–10.9)	0.159
IL-6	9.9	21.5	(1.2–130)	10.1	(0.2–97.2)	0.065
IL-8	24.5	64.7	(10.9–291)	35.1	(6.2–142)	0.156
IL-10	2.76	6.01	(0.8–11.5)	2.81	(0.1–12.0)	0.003
IL-12(p70)	14.6	33.3	(0.6–140)	17.6	(1.4–57)	0.058
IL-13	7.6	13.1	(1.2–33.6)	8.2	(2.7–22.9)	0.015
IL-17	15.7	23.5	(4.6–70)	20.8	(2.1–119)	0.115
Eotaxin	104	141	(51.9–493)	124	(26.3–331)	0.675
G-CSF	7.9	13.2	(2.7–41.3)	8.7	(0.5–17.9)	0.050
IFN-γ	52.6	95.4	(23.1–417)	69.9	(2.5–238)	0.136
MCP-1	20.2	26.8	(8.4–114)	23.8	(3.5–77)	0.744
MIP-1b	97.6	120	(58.3–490)	108	(39.7–263)	0.508
PDGF	4012	4375	(1,312–10,136)	4013	(831–13,557)	0.484
RANTES	2978	2890	(1,040–4,826)	3184	(599–6,165)	0.186
TNF-α	10.5	34.9	(0.1–175)	27.6	(2.9–105)	0.756
VEGF	34.6	101.7	(22.5–371)	59.5	(9.3–183)	0.045

IL interleukin, *G-CSF* granulocytic colony stimulating factor, *IFN* interferon, *MCP* monocyte chemoattractant protein, *MIP* macrophage inflammatory protein, *PDGF* platelet-derived growth factor, *RANTES* regulated upon activation, normal T cell expressed and secreted, *TNF* tumor necrosis factor, *VEGF* vascular endothelial growth factor

Mann–Whitney *U* test was used for univariate analysis of two groups that were classified according to the frequency of MDSCs

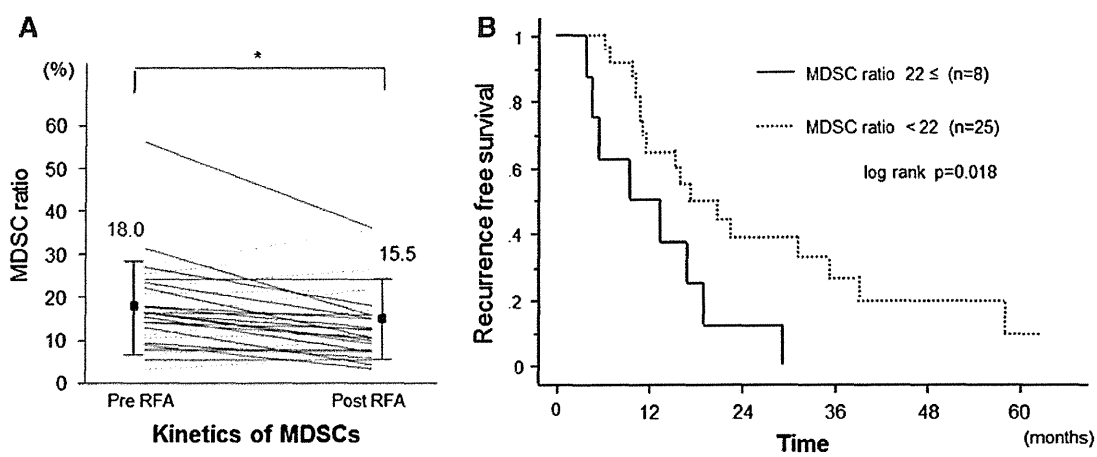

Fig. 3 **a** In 33 HCC patients who received curative RFA therapy, the frequency of MDSCs was significantly decreased after treatment. However, in several patients, the frequencies were increased after treatment (*dotted lines*) (*, $p < 0.05$). **b** Kaplan–Meier curve for recurrence-free survival after RFA therapy. The patients with high frequency of MDSCs (*solid line*) relapsed

concentrations of IL-1ra, IL-2, IL-6, IL-12(p70), and G-CSF tended to be increased in the group with high frequency of MDSCs. In accordance with our results, various cytokines, including IL-6, IL-10, IL-13, G-CSF, and VEGF, that trigger Janus kinase (JAK)-signal transducer and activator of transcription (STAT) signaling pathways have been reported to be associated with the frequency of MDSCs [39]. In particular, the cytokines involved in the JAK2-STAT3 signaling pathway are considered to be the main regulators of the expansion of MDSCs, which leads to stimulation of myelopoiesis and inhibition of myeloid-cell differentiation [40–42].

Table 3 Cox proportional hazards regression for recurrence

Variant	Univariate HR (95 % CI)	*p* value	Multivariable HR (95 % CI)	*p* value
Sex: female	0.763 (0.446–1.308)	0.326		
Age: ≥70 years	1.111 (0.671–1.840)	0.683		
Pre-MDSC ratio: ≥22 %	1.210 (0.698–2.096)	0.497		
Pre-neutrophil	0.990 (0.969–1.012)	0.385		
Pre-lymphocyte	1.014 (0.987–1.043)	0.311		
Pre-neutrophil/lymphocyte	0.978 (0.787–1.216)	0.844		
Pre-ALT	1.001 (0993–1.008)	0.882		
Pre-serum albumin: <3.5 mg/dl	1.143 (0.665–1.982)	0.647		
Pre-prothrombin time: <70 %	1.662 (0.961–2.903)	0.073	1.881 (0.522–6.777)	0.101
Post-MDSC ratio: ≥22 %	2.795 (1.150–6.792)	0.023	3.906 (1.313–11.616)	0.014
Post-neutrophil	1.005 (0.975–1.035)	0.762		
Post-lymphocyte	0.993 (0.960–1.027)	0.678		
Post-neutrophil/lymphocyte	1.003 (0.810–1.242)	0.980		
Post-ALT	0.995 (0.981–1.010)	0.501		
Type IV collagen 7S	1.122 (0.992–1.268)	0.067	1.192 (0.907–1.566)	0.207
AFP: ≥100 ng/ml	1.357 (0.743–2.480)	0.321		
Tumor size: ≥20 mm	1.29 (0.78–2.12)	0.328		
Tumor multiplicity: multiple	2.00 (1.18–3.40)	0.010	1.851 (0.721–4.753)	0.201

HR hazard ratio, *CI* confidence interval, *ALT* alanine aminotransferase, *AFP* alpha-fetoprotein

Another important finding of our study is that the frequency of MDSCs showed various changes after curative RFA and this frequency is an independent risk factor of HCC recurrence. In most of the patients, the frequency of MDSCs decreased after RFA. A similar phenomenon has also been reported in other cancer treatments [19, 21, 36]. Liu et al. [21] reported that MDSCs were decreased in non-small cell lung cancer patients who had clinical benefit from chemotherapy or who received curative surgery. These results suggest that a decrease in the frequency of MDSCs is due to tumor eradication.

It is well known that tumor factors including multiplicity, tumor diameter, serum levels of tumor marker, and hepatic reserve are risk factors of HCC recurrence after RFA [43, 44], but it has not been reported that the frequency of circulating MDSCs is also a risk factor. From our findings, there was a clear inverse correlation between the frequency of MDSCs after RFA and recurrence-free survival. Consistent with our results, in the patients with pancreatic, esophageal, and gastric cancer, Gabitass et al. [23] reported that an increase in MDSCs was associated with an increased risk of death and that the frequency of MDSCs was an independent prognostic factor for patient survival. Taken together with these findings, our results suggest that the frequency of MDSCs might be one of the prognostic factors of patients after cancer treatments.

As we showed, the frequency of MDSCs is primarily correlated with tumor progression. However, between the patients with high and low frequency of MDSCs after RFA, there was no significant difference in hepatic reserve and tumor factors before treatment. Although an incomplete HCC eradication at a microscopic level may allow a high frequency of MDSCs after RFA, there may be other mechanisms such as subsequently tumor-specific immune responses after RFA. In addition, there is a limitation of the present study because we used cryopreserved PBMCs for phenotypic analysis of MDSCs. Further studies using fresh PBMCs are needed for precise phenotypic analysis of MDSCs and elucidation of the mechanism to regulate the frequency of MDSCs after HCC treatment.

In conclusion, the frequency of MDSCs in HCC patients is correlated with tumor progression, and the frequency after RFA is inversely correlated with the prognosis of HCC patients. HCC patients who show a high frequency of MDSCs after RFA should be closely followed, and the inhibition or elimination of MDSCs after HCC treatments may improve the prognosis of HCC patients.

Acknowledgments This study was supported by research grants from the Ministry of Education, Culture, Sports, Science and Technology of Japan.

Conflict of interest The authors declare no conflict of interest.

References

1. Thomas MB, Jaffe D, Choti MM, Belghiti J, Curley S, Fong Y, Gores G (2010) Hepatocellular carcinoma: consensus recommendations of the National Cancer Institute Clinical Trials Planning Meeting. J Clin Oncol 28:3994–4005

2. Llovet JM, Burroughs A, Bruix J (2003) Hepatocellular carcinoma. Lancet 362:1907–1917
3. Lencioni R, Chen XP, Dagher L, Venook AP (2010) Treatment of intermediate/advanced hepatocellular carcinoma in the clinic: how can outcomes be improved? Oncologist 15 Suppl 4:42–52
4. Curley SA, Izzo F, Ellis LM, Nicolas Vauthey J, Vallone P (2000) Radiofrequency ablation of hepatocellular cancer in 110 patients with cirrhosis. Ann Surg 232:381–391
5. Ishizaki Y, Kawasaki S (2008) The evolution of liver transplantation for hepatocellular carcinoma (past, present, and future). J Gastroenterol 43:18–26
6. Yamashita T, Arai K, Sunagozaka H, Ueda T, Terashima T, Mizukoshi E, Sakai A (2011) Randomized, phase II study comparing interferon combined with hepatic arterial infusion of fluorouracil plus cisplatin and fluorouracil alone in patients with advanced hepatocellular carcinoma. Oncology 81:281–290
7. Llovet JM, Ricci S, Mazzaferro V, Hilgard P, Gane E, Blanc JF, de Oliveira AC (2008) Sorafenib in advanced hepatocellular carcinoma. N Engl J Med 359:378–390
8. Butterfield LH (2004) Immunotherapeutic strategies for hepatocellular carcinoma. Gastroenterology 127:S232–S241
9. Sun K, Wang L, Zhang Y (2006) Dendritic cell as therapeutic vaccines against tumors and its role in therapy for hepatocellular carcinoma. Cell Mol Immunol 3:197–203
10. Zerbini A, Pilli M, Penna A, Pelosi G, Schianchi C, Molinari A, Schivazappa S (2006) Radiofrequency thermal ablation of hepatocellular carcinoma liver nodules can activate and enhance tumor-specific T-cell responses. Cancer Res 66:1139–1146
11. Palmer DH, Midgley RS, Mirza N, Torr EE, Ahmed F, Steele JC, Steven NM (2009) A phase II study of adoptive immunotherapy using dendritic cells pulsed with tumor lysate in patients with hepatocellular carcinoma. Hepatology 49:124–132
12. Mizukoshi E, Nakamoto Y, Arai K, Yamashita T, Sakai A, Sakai Y, Kagaya T (2011) Comparative analysis of various tumor-associated antigen-specific t-cell responses in patients with hepatocellular carcinoma. Hepatology 53:1206–1216
13. Whiteside TL (2006) Immune suppression in cancer: effects on immune cells, mechanisms and future therapeutic intervention. Semin Cancer Biol 16:3–15
14. Khattri R, Cox T, Yasayko SA, Ramsdell F (2003) An essential role for Scurfin in CD4 + CD25 + T regulatory cells. Nat Immunol 4:337–342
15. Gabrilovich DI, Nagaraj S (2009) Myeloid-derived suppressor cells as regulators of the immune system. Nat Rev Immunol 9:162–174
16. Zea AH, Rodriguez PC, Atkins MB, Hernandez C, Signoretti S, Zabaleta J, McDermott D (2005) Arginase-producing myeloid suppressor cells in renal cell carcinoma patients: a mechanism of tumor evasion. Cancer Res 65:3044–3048
17. Gordon IO, Freedman RS (2006) Defective antitumor function of monocyte-derived macrophages from epithelial ovarian cancer patients. Clin Cancer Res 12:1515–1524
18. Filipazzi P, Valenti R, Huber V, Pilla L, Canese P, Iero M, Castelli C (2007) Identification of a new subset of myeloid suppressor cells in peripheral blood of melanoma patients with modulation by a granulocyte-macrophage colony-stimulation factor-based antitumor vaccine. J Clin Oncol 25:2546–2553
19. Diaz-Montero CM, Salem ML, Nishimura MI, Garrett-Mayer E, Cole DJ, Montero AJ (2009) Increased circulating myeloid-derived suppressor cells correlate with clinical cancer stage, metastatic tumor burden, and doxorubicin-cyclophosphamide chemotherapy. Cancer Immunol Immunother 58:49–59
20. Brimnes MK, Vangsted AJ, Knudsen LM, Gimsing P, Gang AO, Johnsen HE, Svane IM (2010) Increased level of both CD4 + FOXP3 + regulatory T cells and CD14 + HLA-DR$^-$/low myeloid-derived suppressor cells and decreased level of dendritic cells in patients with multiple myeloma. Scand J Immunol 72:540–547
21. Liu CY, Wang YM, Wang CL, Feng PH, Ko HW, Liu YH, Wu YC (2010) Population alterations of L-arginase- and inducible nitric oxide synthase-expressed CD11b +/CD14$^-$/CD15 +/CD33 + myeloid-derived suppressor cells and CD8 + T lymphocytes in patients with advanced-stage non-small cell lung cancer. J Cancer Res Clin Oncol 136:35–45
22. Vuk-Pavlović S, Bulur PA, Lin Y, Qin R, Szumlanski CL, Zhao X, Dietz AB (2010) Immunosuppressive CD14 + HLA-DRlow/- monocytes in prostate cancer. Prostate 70:443–455
23. Gabitass RF, Annels NE, Stocken DD, Pandha HA, Middleton GW (2011) Elevated myeloid-derived suppressor cells in pancreatic, esophageal and gastric cancer are an independent prognostic factor and are associated with significant elevation of the Th2 cytokine interleukin-13. Cancer Immunol Immunother 60:1419–1430
24. Hoechst B, Ormandy LA, Ballmaier M, Lehner F, Krüger C, Manns MP, Greten TF (2008) A new population of myeloid-derived suppressor cells in hepatocellular carcinoma patients induces CD4(+)CD25(+)Foxp3(+) T cells. Gastroenterology 135:234–243
25. Ostrand-Rosenberg S, Sinha P (2009) Myeloid-derived suppressor cells: linking inflammation and cancer. J Immunol 182:4499–4506
26. Youn JI, Nagaraj S, Collazo M, Gabrilovich DI (2008) Subsets of myeloid-derived suppressor cells in tumor-bearing mice. J Immunol 181:5791–5802
27. Greten TF, Manns MP, Korangy F (2011) Myeloid derived suppressor cells in human diseases. Int Immunopharmacol 11:802–807
28. Filipazzi P, Huber V, Rivoltini L (2011) Phenotype, function and clinical implications of myeloid-derived suppressor cells in cancer patients. Cancer Immunol Immunother 61(2):255–263
29. Ormandy LA, Hillemann T, Wedemeyer H, Manns MP, Greten TF, Korangy F (2005) Increased populations of regulatory T cells in peripheral blood of patients with hepatocellular carcinoma. Cancer Res 65:2457–2464
30. Fu J, Xu D, Liu Z, Shi M, Zhao P, Fu B, Zhang Z (2007) Increased regulatory T cells correlate with CD8 T-cell impairment and poor survival in hepatocellular carcinoma patients. Gastroenterology 132:2328–2339
31. Kusmartsev S, Gabrilovich DI (2006) Effect of tumor-derived cytokines and growth factors on differentiation and immune suppressive features of myeloid cells in cancer. Cancer Metastasis Rev 25:323–331
32. Bunt SK, Sinha P, Clements VK, Leips J, Ostrand-Rosenberg S (2006) Inflammation induces myeloid-derived suppressor cells that facilitate tumor progression. J Immunol 176:284–290
33. Bunt SK, Yang L, Sinha P, Clements VK, Leips J, Ostrand-Rosenberg S (2007) Reduced inflammation in the tumor microenvironment delays the accumulation of myeloid-derived suppressor cells and limits tumor progression. Cancer Res 67:10019–10026
34. Lechner MG, Liebertz DJ, Epstein AL (2010) Characterization of cytokine-induced myeloid-derived suppressor cells from normal human peripheral blood mononuclear cells. J Immunol 185:2273–2284
35. Yuan XK, Zhao XK, Xia YC, Zhu X, Xiao P (2011) Increased circulating immunosuppressive CD14(+)HLA-DR(-/low) cells correlate with clinical cancer stage and pathological grade in patients with bladder carcinoma. J Int Med Res 39:1381–1391
36. Poschke I, Mougiakakos D, Hansson J, Masucci GV, Kiessling R (2010) Immature immunosuppressive CD14 + HLA-DR-/low cells in melanoma patients are Stat3hi and overexpress CD80, CD83, and DC-sign. Cancer Res 70:4335–4345

37. Fattovich G, Stroffolini T, Zagni I, Donato F (2004) Hepatocellular carcinoma in cirrhosis: incidence and risk factors. Gastroenterology 127:S35–S50
38. El-Serag HB, Rudolph KL (2007) Hepatocellular carcinoma: epidemiology and molecular carcinogenesis. Gastroenterology 132:2557–2576
39. Bromberg J (2002) Stat proteins and oncogenesis. J Clin Invest 109:1139–1142
40. Nefedova Y, Huang M, Kusmartsev S, Bhattacharya R, Cheng P, Salup R, Jove R (2004) Hyperactivation of STAT3 is involved in abnormal differentiation of dendritic cells in cancer. J Immunol 172:464–474
41. Yu H, Kortylewski M, Pardoll D (2007) Crosstalk between cancer and immune cells: role of STAT3 in the tumour microenvironment. Nat Rev Immunol 7:41–51
42. Cheng P, Corzo CA, Luetteke N, Yu B, Nagaraj S, Bui MM, Ortiz M (2008) Inhibition of dendritic cell differentiation and accumulation of myeloid-derived suppressor cells in cancer is regulated by S100A9 protein. J Exp Med 205:2235–2249
43. Izumi N, Asahina Y, Noguchi O, Uchihara M, Kanazawa N, Itakura J, Himeno Y (2001) Risk factors for distant recurrence of hepatocellular carcinoma in the liver after complete coagulation by microwave or radiofrequency ablation. Cancer 91:949–956
44. Komorizono Y, Oketani M, Sako K, Yamasaki N, Shibatou T, Maeda M, Kohara K (2003) Risk factors for local recurrence of small hepatocellular carcinoma tumors after a single session, single application of percutaneous radiofrequency ablation. Cancer 97:1253–1262

GASTROENTEROLOGY 2013;145:209–220

BASIC AND TRANSLATIONAL—LIVER

Splenectomy Prolongs the Effects of Corticosteroids in Mouse Models of Autoimmune Hepatitis

RYUTARO MARUOKA,[1,2,*] NOBUHIRO AOKI,[1,2,*] MASAHIRO KIDO,[1,2] SATORU IWAMOTO,[1,2] HISAYO NISHIURA,[1,2] AKI IKEDA,[1,2] TSUTOMU CHIBA,[2] and NORIHIKO WATANABE[1,2]

[1]*Center for Innovation in Immunoregulative Technology and Therapeutics and* [2]*Department of Gastroenterology and Hepatology, Graduate School of Medicine, Kyoto University, Kyoto, Japan*

See Covering the Cover synopsis on page 34.

BACKGROUND & AIMS: Most patients with autoimmune hepatitis (AIH) initially respond to treatment with corticosteroids but often experience a relapse after treatment is withdrawn. BALB/c mice with disruption of programmed cell death 1 (*PD-1*$^{-/-}$ mice) that undergo thymectomy 3 days after birth develop a deregulated immune system, have reduced numbers of Foxp3^{+} regulatory T cells, and develop fulminant hepatic failure that resembles acute-onset AIH in humans. We examined whether splenectomy overcomes corticosteroid insufficiency and reduces the severity of AIH in these mice. We also developed a mouse model of chronic AIH to investigate the effects of splenectomy. **METHODS:** After thymectomy, BALB/c *PD-1*$^{-/-}$ mice were treated with dexamethasone before or after induction of AIH; splenectomy was performed in mice that had and had not been treated with dexamethasone. Neonatal C57BL/6 *PD-1*$^{-/-}$ mice underwent thymectomy to create a model of chronic AIH. **RESULTS:** Injection of dexamethasone before or after induction of AIH prevented development of fatal AIH in BALB/c *PD-1*$^{-/-}$ mice. However, injection of dexamethasone after induction of AIH did not suppress splenic production of follicular helper T cells, and discontinuation of dexamethasone led to a relapse of AIH. Splenectomy (even without administration of dexamethasone) prevented AIH. Neonatal C57BL/6 *PD-1*$^{-/-}$ mice that underwent thymectomy developed chronic hepatitis with fibrosis and hypergammaglobulinemia and produced antinuclear antibodies; AIH was found to be induced in the spleen. Splenectomy reduced liver inflammation in these mice and in BALB/c *PD-1*$^{-/-}$ mice with AIH. **CONCLUSIONS: AIH can be induced in mice via disruption of PD-1 and thymectomy; these cause the same disruptions in immune regulation in BALB/c and C57BL/6 mice but produce different phenotypes. Splenectomy overcomes corticosteroid insufficiency in mice and prolongs the effects of dexamethasone.**

Keywords: Autoimmunity; ANA; Necrosis; T-Cell Response.

Administration of corticosteroids is the first-line therapy for patients with autoimmune hepatitis (AIH). The majority of patients initially respond well to corticosteroids, alone or in combination with azathioprine.[1–4] After initial remission, maintenance therapy is continued for years. However, long-term treatment is discontinued in 13% of patients with AIH because of drug-related side effects.[5,6] Half of patients with AIH who achieve remission experience a relapse within 6 months after withdrawal of corticosteroids, and multiple relapses are associated with a poor prognosis.[7,8] Even when liver inflammation disappears completely, 13% of those patients eventually experience a relapse.[9] In addition to the difficulty in sustaining remission, a recent study showed that the long-term mortality of patients with AIH due to liver disease is greater than that of the general population.[10] Notably, in Europe and the United States, patients with AIH account for 4% of liver transplants.[4] To find clues to overcoming the therapeutic insufficiency of corticosteroids, preclinical animal models for detailed examination are needed.

AIH is characterized by mononuclear cell infiltration in the liver and elevated levels of gamma globulins as well as by the production of a variety of characteristic autoantibodies, including antinuclear antibodies (ANA).[1–3] Liver-infiltrating T cells are considered the primary disease mediators of inflammatory liver damage, and circulating autoantibodies are diagnostic hallmarks.[1–3] However, clinical manifestations are varied in patients with AIH, ranging from nonsymptomatic mild chronic hepatitis to fulminant hepatic failure.[1–3] It is unclear whether the varied clinical manifestations of AIH result from the same immune dysregulation.

Recently, we developed the first mouse model of spontaneous AIH.[11,12] In *programmed cell death 1*–deficient (*PD-1*$^{-/-}$) mice on the BALB/c background that underwent

*Authors share co-first authorship.

Abbreviations used in this paper: AIH, autoimmune hepatitis; ALT, alanine aminotransferase; ANA, antinuclear antibody; AST, aspartate aminotransferase; DEX, dexamethasone; ELISA, enzyme-linked immunosorbent assay; GC, germinal center; HAI, histological activity index; Ig, immunoglobulin; NTx, neonatal thymectomy; NTx-PD-1$^{-/-}$ mice, PD-1–deficient mice that underwent thymectomy 3 days after birth; PBS, phosphate-buffered saline; PD-1, programmed cell death 1; PNA, peanut agglutinin; SD, standard deviation; TCR, T-cell receptor; T_{FH}, follicular helper T; TNF, tumor necrosis factor; Treg, regulatory T cell.

0016-5085/$36.00
http://dx.doi.org/10.1053/j.gastro.2013.03.011

neonatal thymectomy (NTx) 3 days after birth, immune dysregulation by a concurrent loss of naturally arising $Foxp3^+$ regulatory T cells (Tregs) and PD-1–mediated signaling induced fatal AIH resembling acute-onset AIH, presenting in humans as fulminant hepatic failure.[11] The development of fatal AIH was initiated at 2 weeks of age, and extensive destruction of the liver parenchyma resulted in most mice dying by 4 weeks. Fatal AIH in BALB/c-NTx-*PD-1*$^{-/-}$ mice was characterized by $CD4^+$ and $CD8^+$ T-cell infiltration with massive lobular necrosis in the liver, hypergammaglobulinemia, and production of ANA.[11,12] In BALB/c-NTx-*PD-1*$^{-/-}$ mice, fatal AIH was initiated at 2 weeks by splenic follicular helper T (T_{FH}) cells, powerfully assisting B cells in forming germinal centers (GCs).[13] In addition, these T_{FH} cells in the spleen directly migrated into the liver via the CCR6-CCL20 axis, triggering the induction of AIH.[12] However, the development of mouse models of chronic hepatitis similar to the human disease remains an important challenge.

In the present study, using our mouse model of fatal AIH, we examined the effects of administering dexamethasone (DEX) versus splenectomy on the development or progression of AIH. In addition, we developed a new model of chronic AIH. NTx-*PD-1*$^{-/-}$ mice on the different genetic background C57BL/6 developed chronic hepatitis with fibrosis, hypergammaglobulinemia, and the production of ANA, allowing us to examine the effects of administering DEX versus splenectomy.

Materials and Methods

All protocols for mice, administration of DEX *in vivo*, histological and immunohistological analysis, flow cytometry analysis, isolation of lymphocytes, enzyme-linked immunosorbent assay, adoptive transfer, and histological activity index (HAI) scores[14] are detailed in Supplementary Materials and Methods.

Statistical Analysis

The data are presented as the mean values ± standard deviation (SD). Statistical analysis was performed by Student *t* test for unpaired data to compare the values between the 2 groups, and variance was analyzed with the Tukey-Kramer test for multiple comparisons. Survival rates were estimated by the Kaplan-Meier method and compared with the log-rank test. *P* values less than .05 were considered significant.

Results

DEX Prevents the Development of Fatal AIH in BALB/c-NTx-PD-1$^{-/-}$ *Mice*

First, to determine whether corticosteroid therapy prevents AIH in BALB/c-NTx-*PD-1*$^{-/-}$ mice, starting 1 day after thymectomy, the mice were treated intraperitoneally every other day with DEX diluted in phosphate-buffered saline (PBS) or with PBS alone (Figure 1*A*). After 13 injections, mice at 4 weeks of age showed that DEX suppressed severe infiltration of mononuclear cells as well as massive destruction of the liver parenchyma with decreased serum concentrations of aspartate aminotransferase (AST) and alanine aminotransferase (ALT), resulting in a significantly higher survival rate compared with control PBS injections (Figure 1*A* and *B* and Supplementary Figure 1*A*). These data indicate that DEX prevents fatal AIH in these mice.

Therapeutic Administration of DEX Induces Regression of Inflammation in the Liver and Significantly Increases Survival in BALB/c-NTx-PD-1$^{-/-}$ *Mice*

Next, we examined whether corticosteroids might have the same therapeutic efficacy for AIH in BALB/c-NTx-*PD-1*$^{-/-}$ mice as for AIH in humans. Because induction of AIH was started by 14 days of age in most of the mice,[11,12] intraperitoneal injections of DEX were started at 17 days (Figure 1*C*). After 6 injections administered every other day, therapeutic injections of DEX suppressed AIH, inducing significantly greater survival at 4 weeks (Figure 1*C* and *D* and Supplementary Figure 1*B*). These data suggest that similar to AIH in humans, treatment with corticosteroids after induction of AIH is therapeutic for BALB/c-NTx-*PD-1*$^{-/-}$ mice.

Administration of DEX Reduces Serum Immunoglobulin G Levels and Production of ANA in BALB/c-NTx-PD-1$^{-/-}$ *Mice*

Using enzyme-linked immunosorbent assay (ELISA) and immunofluorescence assay, we next examined whether immunoglobulin (Ig) G or ANA levels were affected by preventive or therapeutic injections of DEX. Although serum IgM levels were not changed by treatment with DEX, serum IgG levels were significantly reduced by both preventive and therapeutic injections of DEX (Figure 1*E*). These data are consistent with the finding in patients with AIH that reduced serum AST level after corticosteroid therapy is generally associated with reduced levels of γ-globulin and IgG. In addition, ANA levels were reduced significantly in mice with preventive injections and slightly but not significantly in mice treated with therapeutic injections of DEX (Figure 1*E* and *F*).

Therapeutic Administration of DEX Reduces the Size of the Spleen But Does Not Completely Regress GC-Forming B-Cell Follicles and T_{FH} Cells in the Spleen of BALB/c-NTx-PD-1$^{-/-}$ *Mice*

As reported previously,[12] the spleens of BALB/c-NTx-*PD-1*$^{-/-}$ mice at 4 weeks of age were enlarged, showing multiple peanut agglutinin $(PNA)^+$ GC-forming B-cell follicles. Treatment with DEX significantly reduced spleen size and weight, suggesting that they affect the induction site of development of AIH (Figure 2*A* and Supplementary Figure 2*A* and *B*). However, therapeutic but not preventive DEX injections allowed persistence of multiple B-cell follicles in the spleen (Figure 2*B*, *upper*

BASIC AND TRANSLATIONAL

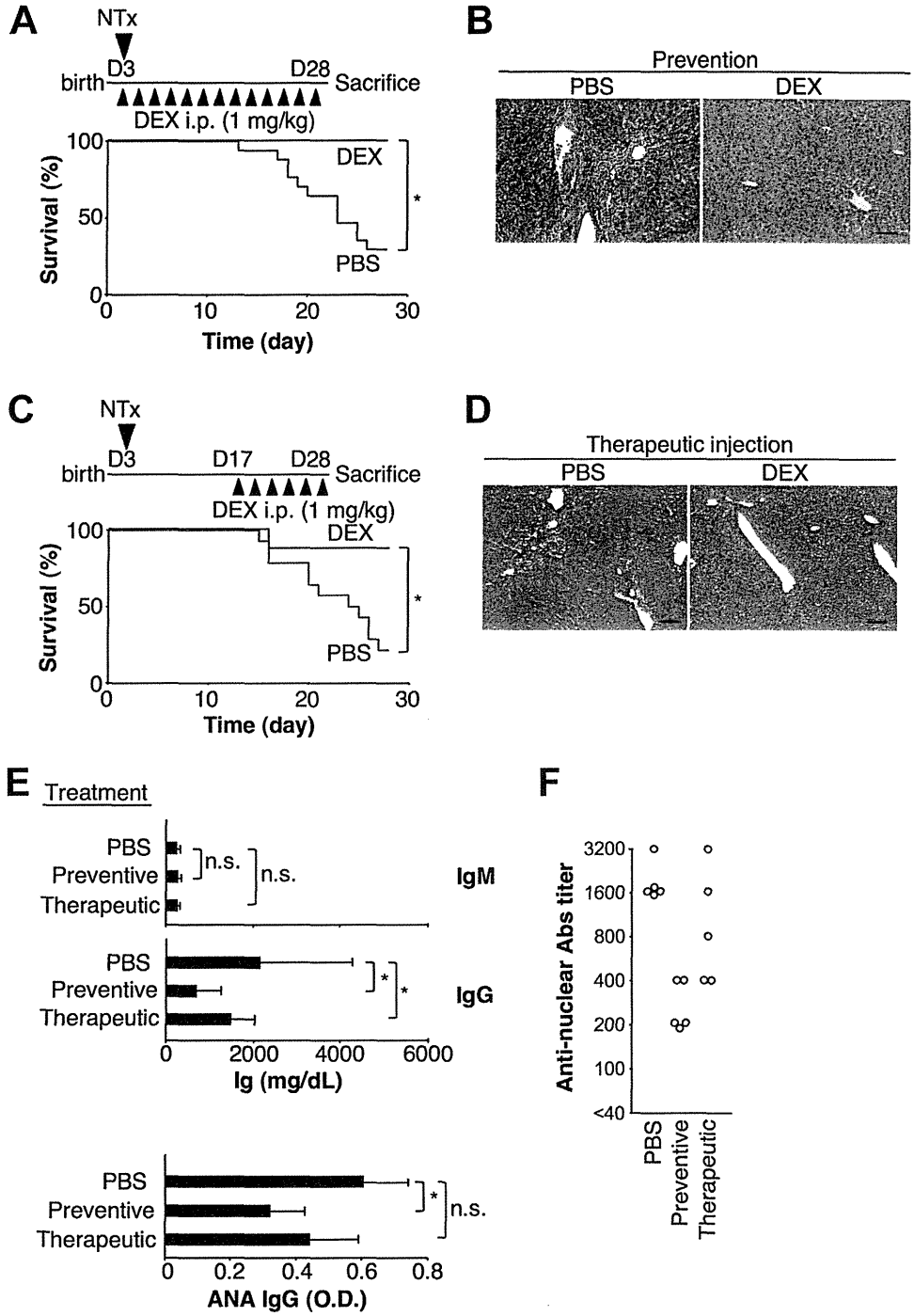

Figure 1. Either preventive or therapeutic injection of DEX suppressed fatal AIH in BALB/c-NTx-*PD-1*$^{-/-}$ mice. (*A*, *B*, *E*, *F*) With preventive injections, mice at 1 day after thymectomy were intraperitoneally injected every other day with 1.0 mg/kg DEX diluted in PBS (n = 5) or PBS alone (n = 17). After 13 injections, mice at 4 weeks of age were killed. (*C–F*) With therapeutic injections, mice at 14 days after thymectomy were injected every other day with DEX (n = 11) or PBS alone (n = 13). After 6 injections, mice at 4 weeks of age were killed. (*A* and *C*) Survival rate. (*B* and *D*) Liver staining with H&E. (*E*) Serum levels of IgM, IgG, and ANA measured by ELISA. (*F*) Serum titers of ANAs. *Open circles* indicate the maximum dilution of sera from individual mice as detected by fluorescence immunohistology. *Bars* indicate the mean of each group, and the *error bars* indicate SD. *$P < .05$. All *scale bars* = 100 μm. n.s., not significant.

panels) and of CD4$^+$ T_{FH} cells as well as PNA$^+$ GC formation in the B220$^+$ B-cell follicles (Figure 2*B*, *middle and lower panels*) in the spleens of BALB/c-NTx-*PD-1*$^{-/-}$ mice aged 4 weeks. In addition, flow cytometric analysis of splenic CD4$^+$ T cells showed that these cells in mice therapeutically treated with DEX contained ICOS$^+$CXCR5$^+$ T_{FH} cells at levels similar to those of controlled mice treated with PBS. In contrast, ICOS$^+$CXCR5$^+$ T_{FH} cells in CD4$^+$ T-cell populations were reduced in mice preventively treated with DEX (Figure 2*C*). Although injections of DEX may affect immune cells other than T cells in the spleen, therapeutic injections of DEX allowed T_{FH} cells to persist.

Corticosteroids directly induce apoptosis of lymphocytes, whereas Tregs expressing higher levels of glucocorticoid receptors are reported to be resistant to DEX-mediated apoptosis, probably due to high expression of Bcl-2.[15–17] We next examined whether splenic CD4$^+$ T cells containing T_{FH} cells are more resistant

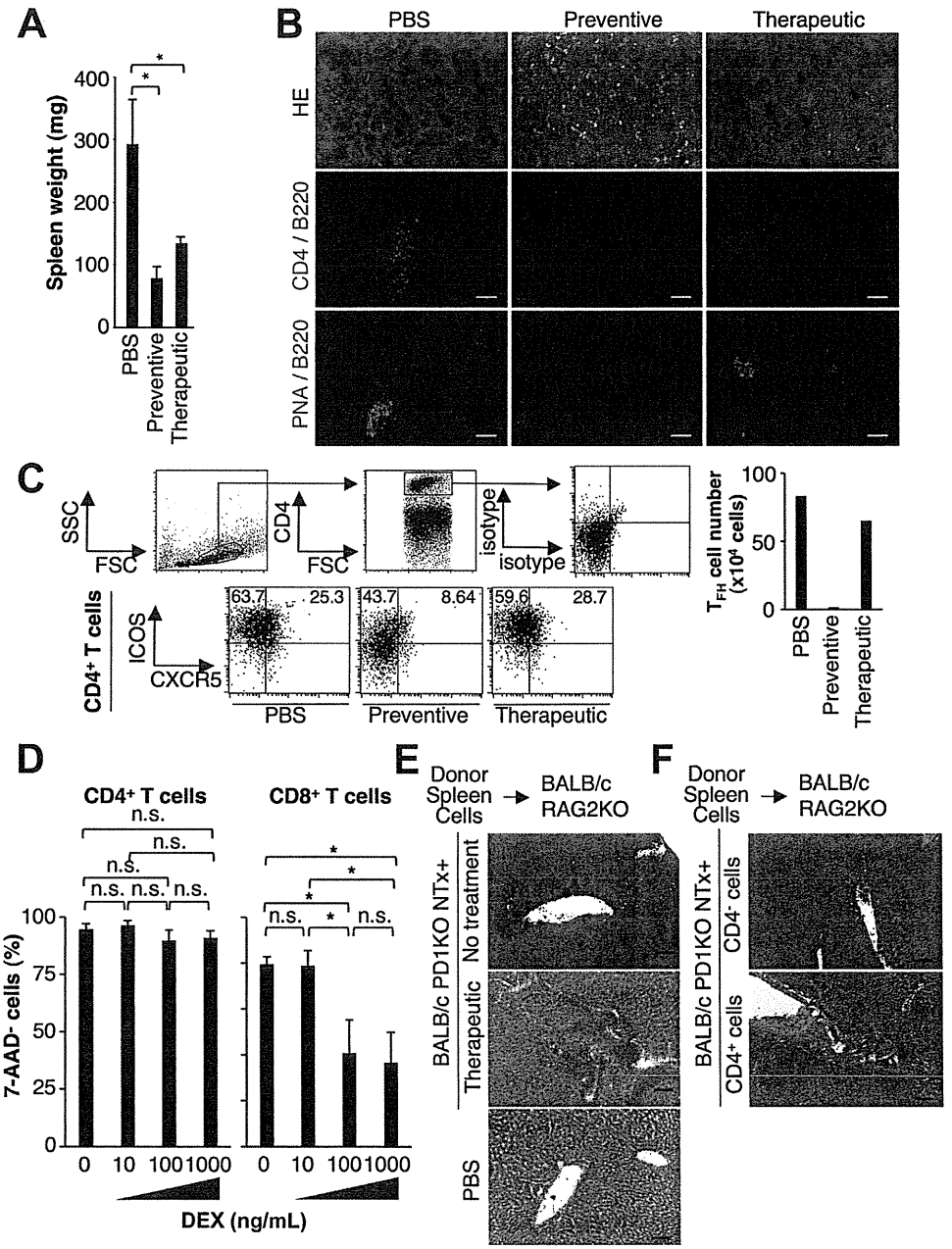

Figure 2. Therapeutic administration of DEX reduces spleen weight but does not completely regress T_{FH} cells in the spleen of BALB/c–NTx–*PD-1*$^{-/-}$ mice. Mice were treated with DEX or PBS alone preventively or therapeutically, as described in Figure 1. (*A*) Spleen weights. (*B*) Histological analysis of the spleens from each group with H&E staining. *Arrowheads* indicate follicles. Spleens from each group were immunohistologically stained for CD4, PNA (*green*), and B220 (*red*). (*C*) Flow cytometric analysis of splenic $CD4^+$ T cells from each group. The numbers in the plots indicate the percentage of $ICOS^+CXCR5^+$ and $ICOS^+CXCR5^-$ cells in the $CD4^+$ T-cell population (*left panels*). The numbers of $ICOS^+CXCR5^+$ $CD4^+$ T (T_{FH}) cells were calculated as follows: (Percentage of Cells in Viable Cells) × (Number of Viable Cells) (*right panel*). (*D*) Flow cytometric analysis of $CD4^+$ and $CD8^+$ T cells. Spleen cells of mice injected with DEX therapeutically were cultured for 3 days with anti-CD3 and anti-CD28 monoclonal antibodies and the indicated concentration of DEX. The percentages of 7-AAD$^-$ cells in $CD3^+CD4^+$ and $CD3^+CD8^+$ T cells are shown. Data represent one of 3 separate experiments. (*E* and *F*) Staining with H&E of the livers from recipient BALB/c-*RAG2*$^{-/-}$ mice at 3 weeks after transfer. (*E*) Total splenocytes were isolated and intravenously transferred from BALB/c–NTx–*PD-1*$^{-/-}$ mice with or without therapeutic injections of DEX. (*F*) Purified splenic $CD4^+$ T cells or $CD4^+$ T cell–depleted splenocytes ($CD4^-$ cells) were transferred from BALB/c–NTx–*PD-1*$^{-/-}$ mice therapeutically treated with DEX. *Bars* indicate the mean of each group, and the *error bars* indicate SD. *$P < .05$. n.s., not significant. *Scale bars* = 100 μm.

to DEX-mediated apoptosis than other T cells. $CD4^+$ and $CD8^+$ T cells were purified from the spleen of BALB/c–NTx–*PD-1*$^{-/-}$ mice therapeutically treated with DEX and cultured with various concentrations of DEX (Figure 2*D*). After 3 days of culture, 7-AAD$^-$ nonapoptotic cells were significantly and dose-dependently reduced in the $CD8^+$ T-cell population cultured with DEX. In contrast, 7-AAD$^-$ nonapoptotic cells were not altered

in the $CD4^+$ T-cell population cultured with DEX (Figure 2*D*). These data suggest that in BALB/c-NTx-*PD-1*$^{-/-}$ mice, splenic $CD4^+$ T cells containing T_{FH} cells are more resistant to DEX-mediated apoptosis than effector $CD8^+$ T cells.

Residual Splenic $CD4^+$ Cells After Therapeutic Injections of DEX Can Induce Hepatitis in RAG2$^{-/-}$ *Mice*

Next, we investigated whether residual splenic $CD4^+$ cells after therapeutic injections of DEX can induce AIH. Total splenocytes, purified splenic $CD4^+$ cells, or $CD4^+$ T cell-depleted splenocytes were transferred from BALB/c-NTx-*PD-1*$^{-/-}$ mice therapeutically treated with DEX at 3 weeks into T cell- and B cell-deficient BALB/c-*RAG2*$^{-/-}$ mice. Three weeks later, we found that transferring total splenocytes from mice therapeutically treated with DEX induced mononuclear cell infiltrations in the liver of recipient mice and significantly increased serum levels of AST and ALT to levels similar to those of untreated mice (Figure 2*E* and Supplementary Figure 2*C*). Notably, purified splenic $CD4^+$ T cells but not $CD4^+$ T cell-depleted splenocytes also induced hepatitis (Figure 2*F* and Supplementary Figure 2*D*). Taken together, these data suggest that residual splenic $CD4^+$ cells trigger the recurrence of AIH in mice after treatment with DEX.

Discontinuing Therapy with DEX Induces Fatal Hepatitis, Whereas Extending It Allows Residual GC-Forming B-Cell Follicles in the Spleen of BALB/c-NTx-PD-1$^{-/-}$ *Mice*

To examine whether discontinuing treatment with DEX results in relapse, administration of DEX ended at 28 days of age after 6 therapeutic injections or continued until 40 days of age in control mice (Figure 3*A*). Continuous treatment with DEX maintained suppressed inflammatory infiltration in the liver and hepatic damage in association with a high survival rate (Figure 3*A* and *B* and Supplementary Figure 3), but GC-forming B-cell follicles were still present in the spleen (Figure 3*B*). In contrast, stopping treatment with DEX at 28 days resulted in the recurrence of hepatitis at 40 days, accompanied by reduced survival rates (Figure 3*A* and *B* and Supplementary Figure 3). These data suggest a limitation in the therapeutic use of corticosteroids for resolving the dysregulation of T_{FH} cells in the spleen, the induction site of AIH, in BALB/c-NTx-*PD-1*$^{-/-}$ mice.

Splenectomy After the Development of AIH Suppresses Progression to Fatal AIH in BALB/c-NTx-PD-1$^{-/-}$ *Mice*

Previously we reported that neonatal splenectomy has a preventive effect on the development of AIH in BALB/c-NTx-*PD-1*$^{-/-}$ mice.[12] In this study, we evaluated splenectomy as a therapeutic option. Similar to the neonatal procedure, splenectomy at 7 or 10 days of age before induction of AIH suppressed the development of fatal hepatitis (Figure 3*C*). Importantly, we found that splenectomy at 17 or 21 days of age after development of AIH also suppressed liver inflammation and improved survival, sustaining remission until 45 days (Figure 3*C–E*).

In addition, splenectomy at 21 days of age after treatment with DEX suppressed liver inflammation in association with a high survival rate at 40 days of age, sustaining remission until 60 days (Figure 3*F*). Moreover, when we performed splenectomy at 4 weeks of age after treatment with DEX, liver inflammation was suppressed at 56 days of age (Supplementary Figure 4). These data suggest that splenectomy induces prolonged remission of AIH in BALB/c-NTx-*PD-1*$^{-/-}$ mice.

AIH That Develops in C57BL/6-NTx-PD-1$^{-/-}$ *Mice Shares Characteristic Components of Chronic Hepatitis in Patients With AIH*

Clinical manifestations of AIH are varied in patients with AIH, and the disease manifestation has been associated with specific alleles of the major histocompatibility complex.[1-3,18,19] To test whether different genetic backgrounds induce milder disease manifestation in NTx-*PD-1*$^{-/-}$ mice, we performed NTx in *PD-1*$^{-/-}$ mice that had been backcrossed onto the C57BL/6 background for 11 generations.[20]

In 2-week-old BALB/c-NTx-*PD-1*$^{-/-}$ mice with hepatitis, pathogenic splenic T_{FH} cells were preferentially localized within $B220^+$ B-cell follicles and autonomously developed PNA^+ GCs (Supplementary Figure 5).[12] In contrast, although splenic $CD4^+$ T cells were located within the follicles in C57BL/6-NTx-*PD-1*$^{-/-}$ mice of the same age, these B-cell follicles did not develop PNA^+ GCs (Supplementary Figure 5 and Figure 4*A*). Interestingly, flow cytometric analysis showed that in parallel to the increase in $ICOS^+CD4^+$ T cells, including $CXCR5^+$ T_{FH} cells, in C57BL/6-NTx-*PD-1*$^{-/-}$ mice at 6 weeks of age (Supplementary Figure 6*A*), PNA^+ GCs autonomously developed (Figure 4*A*) and $B220^+$ B cells expressed Fas and GL7 (Figure 4*B*), hallmarks of GC B cells. Importantly, livers in C57BL/6-NTx-*PD-1*$^{-/-}$ mice as young as 4 weeks showed mononuclear cell infiltrations, predominantly in the portal area. The infiltration was sustained in older mice, resulting in bridging fibrosis (Figure 4*C* and *D vii* and *viii* and Supplementary Figure 6*B*). Histological examination of the liver in 8-week-old C57BL/6-NTx-*PD-1*$^{-/-}$ mice showed interface hepatitis with periportal necrosis without bile duct destruction (Figure 4*D*, *i–iii*), intralobular degeneration (Figure 4*D*, *iv*), or portal inflammation (Figure 4*D*, *v*) as well as fibrosis (Figure 4*D*, *vi*). These findings are associated with an increased HAI score and increased serum levels of AST and ALT (Figure 4*E* and Supplementary Figure 6*C*).

In addition, C57BL/6-NTx-*PD-1*$^{-/-}$ mice older than 4 weeks had hypergammaglobulinemia and significantly increased production of ANAs as detected by ELISA and immunofluorescence assay (Figure 5*A–C*). All C57BL/6-NTx-*PD-1*$^{-/-}$ mice older than 8 weeks developed AIH, whereas some of the AIH-bearing mice, at a lesser frequency, manifested other organ-specific autoimmunity

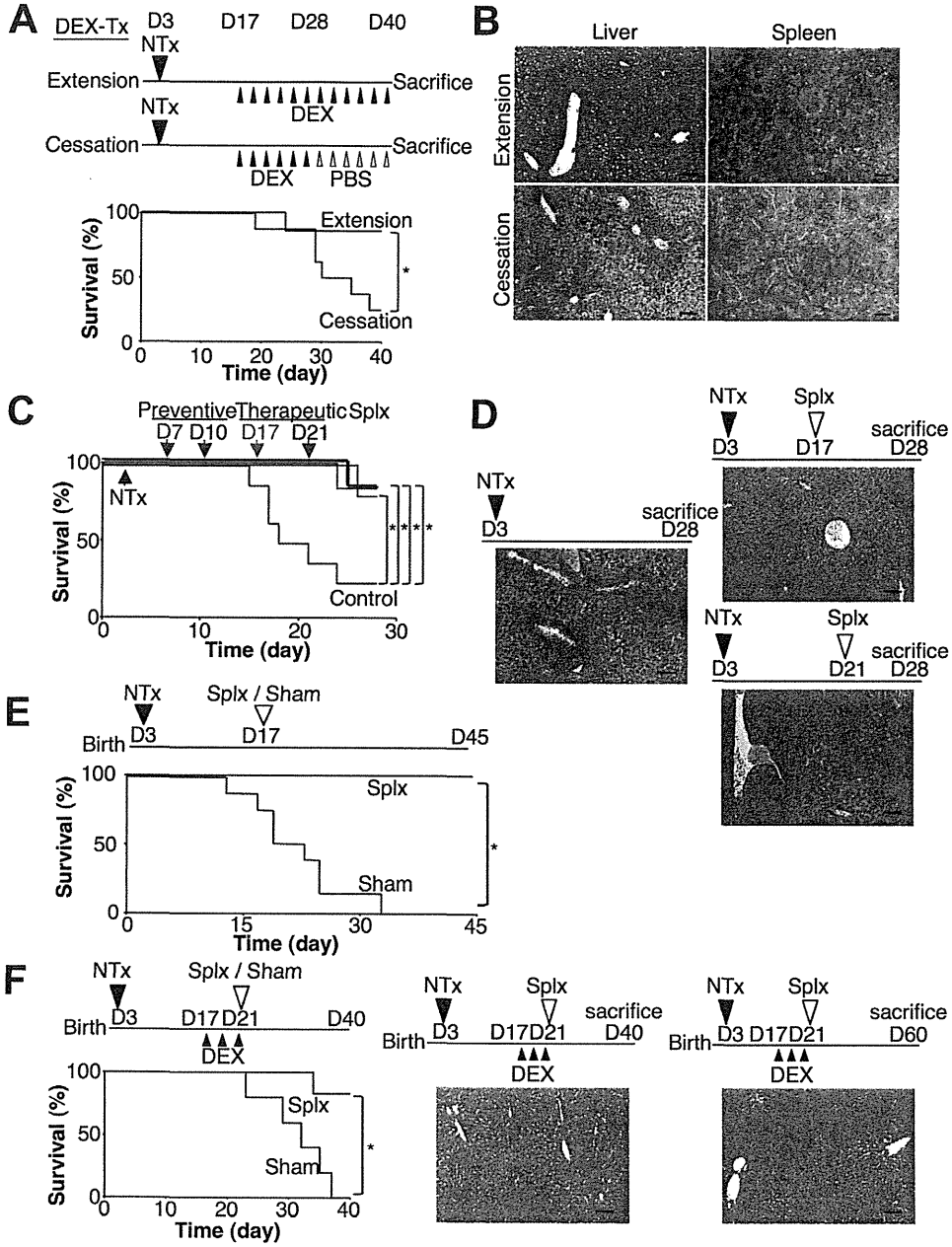

Figure 3. Splenectomy overcomes the therapeutic insufficiency of corticosteroids and induces prolonged remission of AIH in BALB/c-NTx-*PD-1*$^{-/-}$ mice. (*A* and *B*) Mice were treated with DEX therapeutically, as described in Figure 1. Mice that received injections of DEX until 40 days of age (Extension, n = 7) and mice that underwent cessation of DEX injections at 4 weeks of age (Cessation, n = 10) were killed at 40 days of age. (*A*) Survival rate of each group. (*B*) Staining of the liver and spleen with H&E. (*C* and *D*) Splenectomy (Splx) was performed on BALB/c-NTx-*PD-1*$^{-/-}$ mice at 7 (n = 6) or 10 days (n = 5) before induction and 17 (n = 6) or 21 days of age (n = 6) after development of AIH. (*C*) The survival rate of each group and (*D*) liver staining with H&E at 28 days of age. (*E*) The survival rate at 45 days of age in BALB/c-NTx-*PD-1*$^{-/-}$ mice undergoing splenectomy (Splx, n = 8) or sham operation (Sham, n = 8) at 17 days of age. (*F*) Mice were treated with DEX therapeutically, as described in Figure 1. After 3 injections, mice stopped receiving DEX injections and underwent splenectomy (Splx, n = 6) or sham operation (n = 5) at 21 days of age. The survival rate of each group is shown in the *left panel*. Splx mice were killed at 40 days of age, and the livers were harvested. Liver staining with H&E is shown in the *middle panel*. For the experiment in *F* (*right panel*), indicated mice were killed at 60 days (n = 3). *$P < .05$. All *scale bars* = 100 μm.

such as sialadenitis, as did patients with chronic AIH (Figure 5*D* and Supplementary Table 1).[1-3] These data suggest that chronic AIH in humans and AIH that developed in C57BL/6-NTx-*PD-1*$^{-/-}$ mice share characteristic components of the disease.

Chronic Hepatitis That Developed in C57BL/6-NTx-PD-1$^{-/-}$ *Mice Is Organ-Specific Autoimmunity Induced by CD4*$^{+}$ *T Cells*

In 6-week-old C57BL/6-NTx-*PD-1*$^{-/-}$ mice, flow cytometric analysis showed that CD3^{+} T cells predominantly infiltrated the liver. These cells were mainly CD8^{+} T cells and, to a lesser extent, CD4^{+} T cells, as described for BALB/c-NTx-*PD-1*$^{-/-}$ mice (Figure 5*E* and *F*).[11] These results were further confirmed by immunohistology (Figure 6*A*). In BALB/c-NTx-*PD-1*$^{-/-}$ mice, CD4^{+} T cells in the enlarged spleen directly triggered development of AIH.[12] Although adult C57BL/6-NTx-*PD-1*$^{-/-}$ mice did not show obvious splenomegaly (Figure 6*B* and Supplementary Figure 7), transfer of splenic CD4^{+} T cells from AIH-bearing C57BL/6-NTx-*PD-1*$^{-/-}$ mice at 8 weeks of age into T cell- and B cell-deficient *RAG2*$^{-/-}$ mice induced hepatitis in recipient mice at 3 weeks after transfer (Figure 6C). These data suggest that splenic CD4^{+} T cells directly trigger AIH in this chronic model.

BASIC AND TRANSLATIONAL

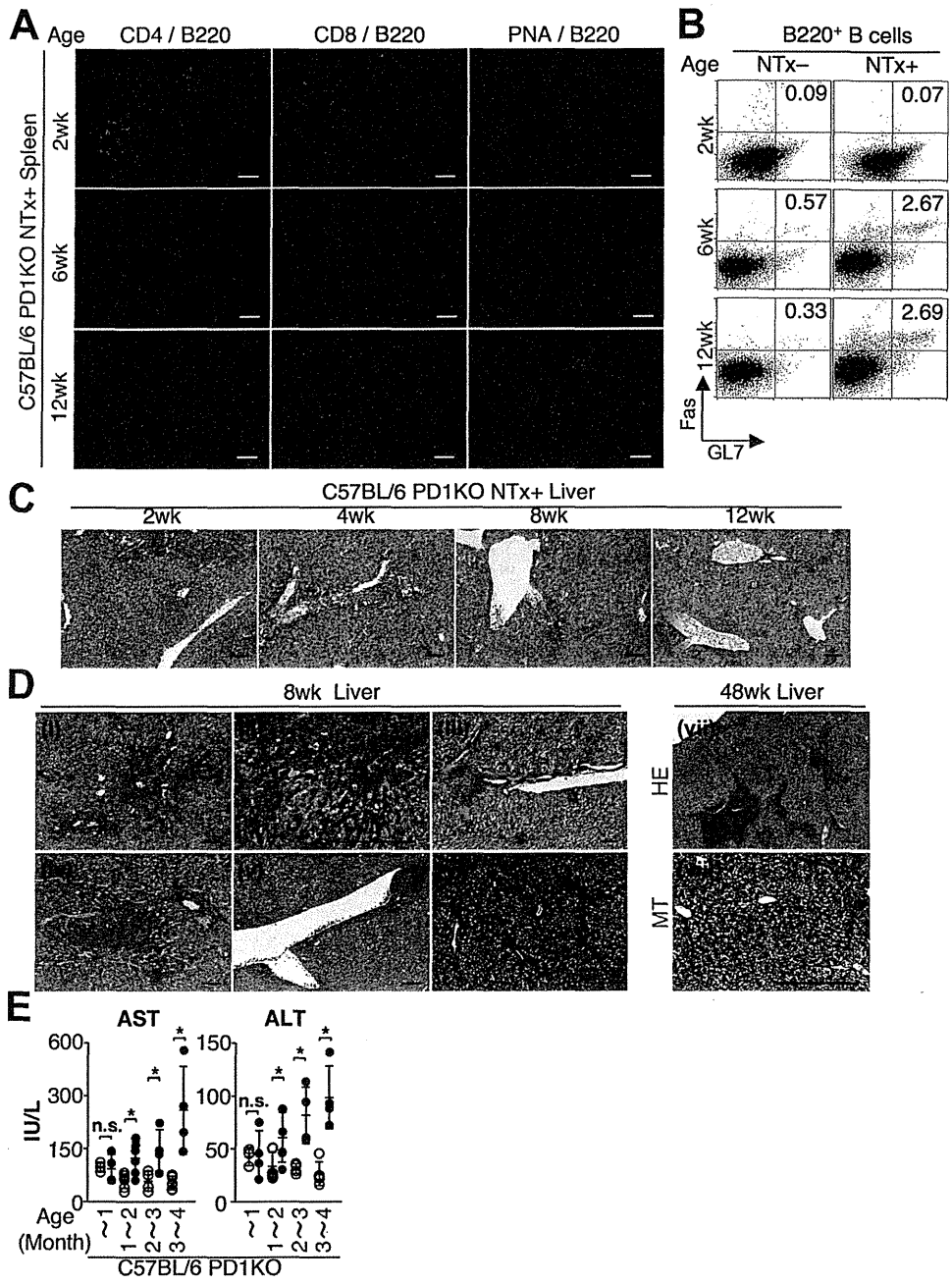

Figure 4. Adult C57BL/6-NTx-*PD-1*$^{-/-}$ mice spontaneously develop B220^{+}PNA^{+} GCs with CD4^{+} T_{FH} cells in the spleen and have chronic hepatitis with fibrosis. (*A*) Immunohistological staining of spleens in indicated mice at 2 to 12 weeks. The spleens were stained for CD4, CD8, PNA (*green*), and B220 (*red*). (*B*) Flow cytometric analysis of splenic B cells in indicated mice. The numbers in plots indicate the percentage of B220^{+}Fas^{+}GL7^{+} GC B cells. (*C*) Liver staining with H&E in C57BL/6-NTx-*PD-1*$^{-/-}$ mice at 2 to 12 weeks. (*D*) Liver staining with H&E for 8-week-old (*left panels, i–v*) and 48-week-old mice (HE, *right panels*). Masson's trichrome staining of livers from 8-week-old (*left panel, vi*) and 48-week-old mice (MT, *right panels*). (*E*) Serum levels of AST and ALT in C57BL/6-*PD-1*$^{-/-}$ mice at indicated ages with (*closed circles*) or without NTx (*open circles*). *Bars* indicate the mean of each group, and the *error bars* indicate SD. *$P < .05$. n.s., not significant. All *scale bars* = 100 μm.

In addition, using ELISA sets for cytokines, we found that serum cytokine levels of tumor necrosis factor (TNF)-α but not interferon gamma increased in 6-week-old C57BL/6-NTx-*PD-1*$^{-/-}$ mice (Figure 6*D*). Furthermore, when we transferred splenic CD4^{+} T cells from AIH-bearing C57BL/6-NTx-*PD-1*$^{-/-}$ mice as described previously (Figure 6*C*), transferred CD4^{+} T cells not only induced hepatitis but also elevated serum levels of TNF-α in recipient mice (Figure 6*E*). Because TNF-α directly and indirectly induces cell death of hepatocytes,[21] TNF-α may be involved in hepatocytic damage in C57BL/6-NTx-*PD-1*$^{-/-}$ mice.

Analysis of the T-cell receptor (TCR) repertoire in several autoimmune diseases has shown antigen-driven clonal expansion of autoreactive T cells in the target organs.[22–26] In patients with AIH, analyses of the TCR repertoire have shown skewing of V_β chain use, suggesting oligoclonal expansion of liver-infiltrating T cells.[27,28] In addition, liver-infiltrating LKM-1–specific CD4^{+} T-cell clones have shown a restricted TCR V_β repertoire.[29] To determine the clonality of infiltrating CD4^{+} T cells in the liver, we used flow cytometry to examine the TCR V_β usage of hepatic CD4^{+} T cells. Broad TCR V_β usages were equivalent to hepatic CD4^{+} T cells in wild-type mice and *PD-1*$^{-/-}$ mice without NTx (Figure 6*F*, *upper and middle panels*). In contrast, in 6-week-old C57BL/6-NTx-*PD-1*$^{-/-}$ mice, effector T cells infiltrated into the liver showed clonal expansion (Figure 6*F*, *lower left panel*). Interestingly,

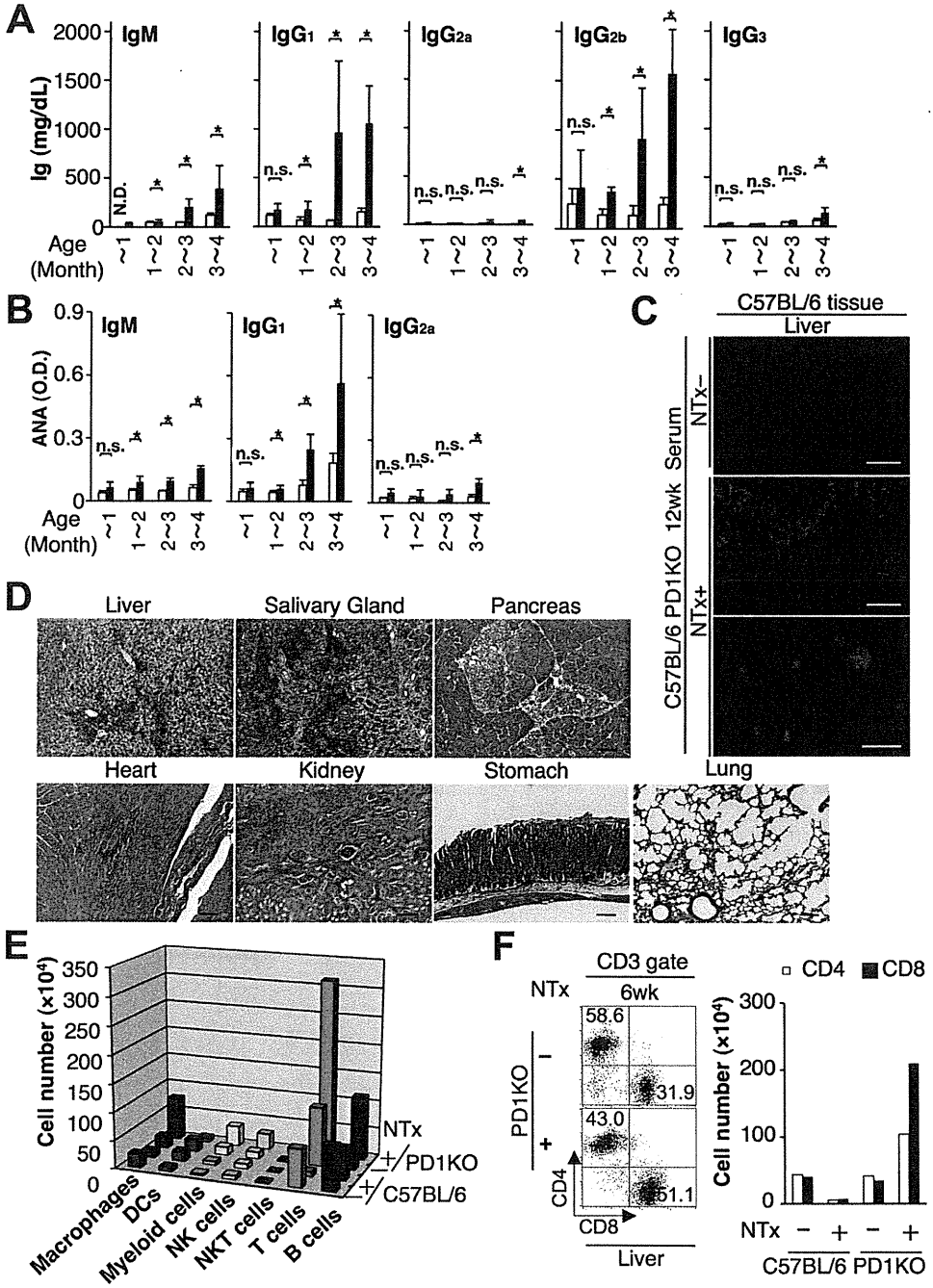

Figure 5. Adult C57BL/6-NTx-*PD-1*$^{-/-}$ mice develop hypergammaglobulinemia, ANA production, and autoimmunity in other organs, and T cells are predominantly infiltrated in the inflamed liver. (*A* and *B*) The serum levels of (*A*) total Ig subclasses and (*B*) ANA subclasses determined by ELISA are shown. Data shown are from C57BL/6-*PD-1*$^{-/-}$ mice at indicated ages with (*closed bars*) or without NTx (*open bars*). *Bars* indicate the mean of each group, and the *error bars* indicate the SD. *$P < .05$. N.D., not detected. n.s., not significant. (*C*) Autoantibodies detected by fluorescence immunohistology as described in Supplementary Materials and Methods. Sera (100× diluted) from 12-week-old C57BL/6-*PD-1*$^{-/-}$ mice with or without NTx were used. *Scale bars* = 100 μm (*upper and middle panels*) or 10 μm (*lower panel*). (*D*) Histological findings of various organs from 12-week-old C57BL/6-NTx-*PD-1*$^{-/-}$ mice. *Scale bars* = 100 μm. (*E*) Cell numbers of each subset of liver mononuclear cells as described in Supplementary Materials and Methods. Data represent the numbers in the indicated mice at 6 weeks of age. (*F*) Flow cytometric analysis (*left panel*) and cell numbers (*right panel*) of $CD3^+CD4^+$ and $CD3^+CD8^+$ T cells in the liver of 6-week-old C57BL/6-*PD-1*$^{-/-}$ mice with or without NTx. The numbers in the quadrants indicate the percentage of cells in that gate (*left panel*). Data shown in *C*, *E*, and *F* are from one of 3 separate experiments.

in the case of fatal hepatitis in 3-week-old BALB/c-NTx-*PD-1*$^{-/-}$ mice, effector T cells infiltrated into the liver showed more abundant clonal expansion, probably affecting the severity of inflammation (Figure 6*F*, *lower right panel*). These data suggest that monoclonal or oligoclonal expansion of infiltrating effector $CD4^+$ T cells in the liver may be relevant to the proliferation of autoreactive $CD4^+$ T cells induced by autoantigen-presenting dendritic cells in the spleen.

In addition, in C57BL/6-NTx-*PD-1*$^{-/-}$ mice, we found that infiltrates in the liver were less likely to contain Tregs (Supplementary Figure 8*A*). Previously, we showed that in BALB/c-NTx-*PD-1*$^{-/-}$ mice, the transfer of Tregs could not suppress progression of fatal hepatitis after the induction of AIH.[11] However, when Tregs isolated from splenocytes of adult C57BL/6-*PD-1*$^{-/-}$ mice (Supplementary Figure 8*B*) were transferred into 4-week-old C57BL/6-NTx-*PD-1*$^{-/-}$ mice, the transfer suppressed chronic AIH (Supplementary Figure 8*C–E*). In humans, Tregs in peripheral blood have the same suppressive activity as Tregs isolated from the spleen in mice.[30–32] Thus, Tregs isolated from peripheral blood and expanded ex vivo might be able to suppress AIH in humans.

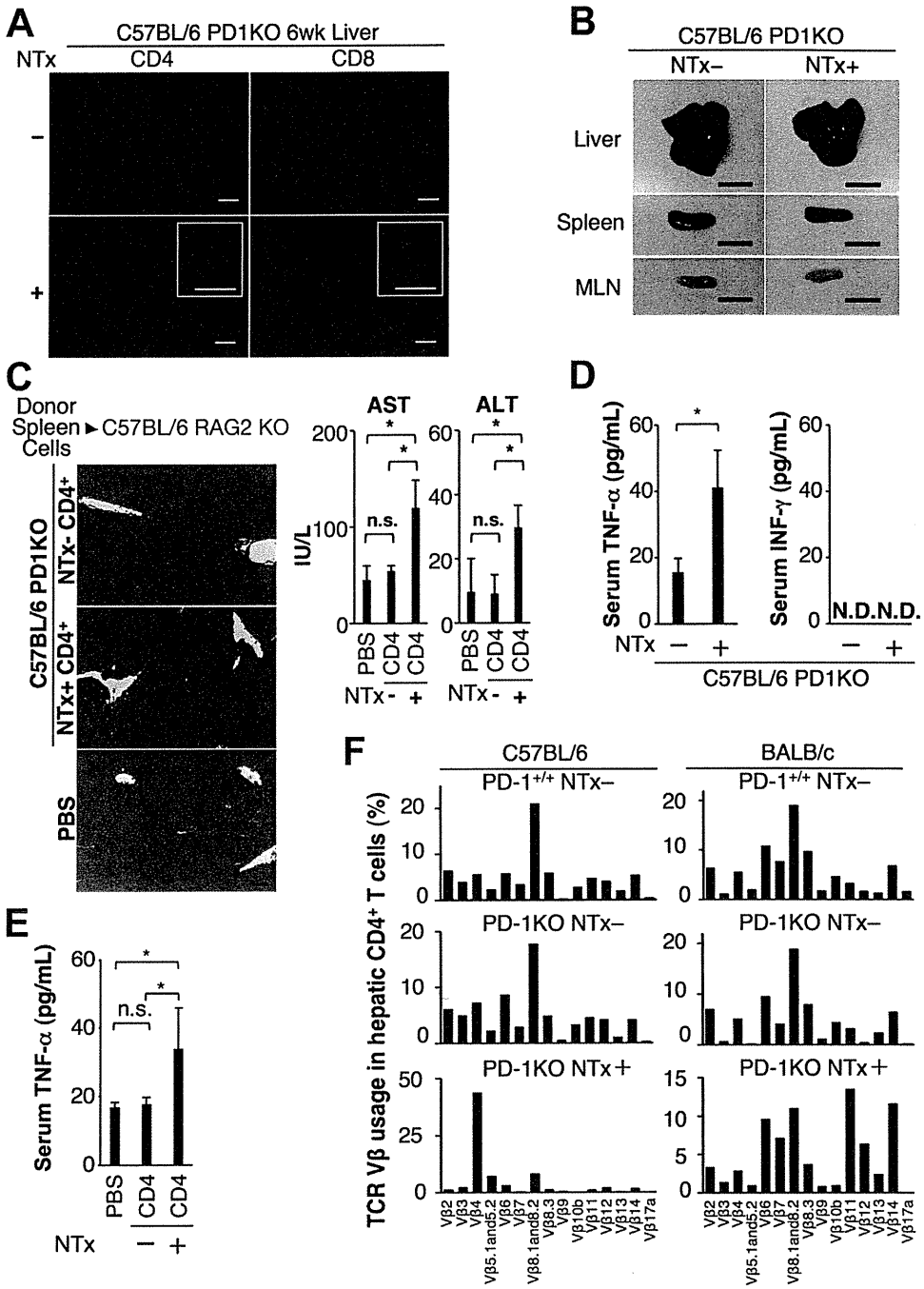

Figure 6. Splenic $CD4^+$ T cells are responsible for induction of chronic AIH, and $CD4^+$ T cells infiltrated in the liver show clonal expansion in NTx-*PD-1*$^{-/-}$ mice. (*A*) Immunohistological staining of livers. The livers in 6-week-old C57BL/6-*PD-1*$^{-/-}$ mice with or without NTx were stained with fluorescein isothiocyanate anti-CD4 or anti-CD8. The *insets* show staining for CD4 or CD8 with a higher magnification. *Scale bars* = 100 μm. (*B*) Macroscopic view of the liver, spleen, and mesenteric lymph node (MLN) from 12-week-old indicated mice. *Scale bars* = 1 cm. (*C*) Purified $CD3^+CD4^+$ T cells from the spleen of 8-week-old C57BL/6-*PD-1*$^{-/-}$ mice with or without NTx were transferred into *RAG2*$^{-/-}$ mice intravenously. Three weeks after transfer, recipient mice were examined. Liver staining with H&E. *Scale bars* = 100 μm (*left panel*). Serum levels of the liver transaminases AST and ALT (*right panel*). (*D*) Serum levels of TNF-α and interferon gamma (INF-γ) in 6-week-old indicated mice as measured by ELISA. (*E*) Serum levels of TNF-α in recipient mice transferred as described in *C*. (*F*) TCR V_β usages of hepatic $CD4^+$ T cells in indicated mice assessed by flow cytometry. Mononuclear cells in the liver were stained as described in Supplementary Materials and Methods. Data shown are from one of 3 separate experiments. The *bars* in *C–E* indicate the mean of each group, and the *error bars* indicate SD. *$P < .05$. n.s., not significant; N.D., not detected.

The Spleen Is the Induction Site of AIH in C57BL/6–NTx–PD-1$^{-/-}$ *Mice, and Splenectomy Suppresses Chronic AIH Similar to Fulminant AIH*

C57BL/6-NTx-*PD-1*$^{-/-}$ mice at 4 weeks of age showed mononuclear cell infiltrations in the liver and increased serum levels of AST and ALT (Figures 4*C* and 7*A*). To examine whether corticosteroids have therapeutic efficacy for chronic AIH in C57BL/6-NTx-*PD-1*$^{-/-}$ mice as in human AIH, intraperitoneal injections of DEX were started at 4 weeks (Figure 7*B*). After 14 injections every other day until 8 weeks of age, therapeutic injections of DEX suppressed AIH (Figure 7*B* and Supplementary Figure 9).

As in BALB/c-NTx-*PD-1*$^{-/-}$ mice, neonatal splenectomy also suppressed AIH in C57BL/6-NTx-*PD-1*$^{-/-}$ mice (Figure 7*C* and Supplementary Figure 10*A* and *B*), suggesting that the spleen is the induction site for chronic development of AIH in C57BL/6-NTx-*PD-1*$^{-/-}$ mice.

Finally, we evaluated splenectomy as a therapeutic option in 4-week-old mice. Similar to the neonatal procedure, splenectomy at 4 weeks suppressed AIH in

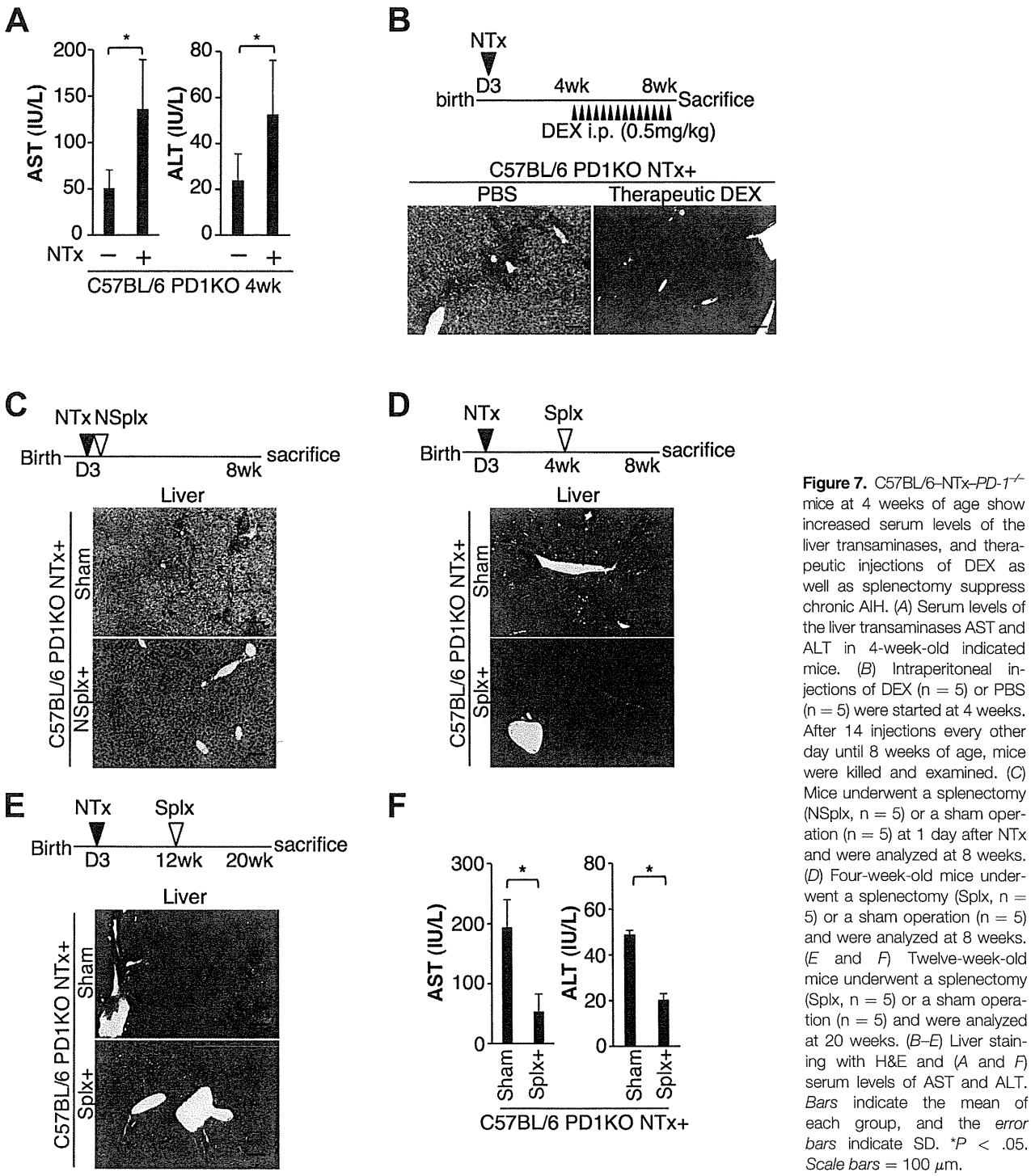

Figure 7. C57BL/6-NTx-*PD-1*$^{-/-}$ mice at 4 weeks of age show increased serum levels of the liver transaminases, and therapeutic injections of DEX as well as splenectomy suppress chronic AIH. (*A*) Serum levels of the liver transaminases AST and ALT in 4-week-old indicated mice. (*B*) Intraperitoneal injections of DEX (n = 5) or PBS (n = 5) were started at 4 weeks. After 14 injections every other day until 8 weeks of age, mice were killed and examined. (*C*) Mice underwent a splenectomy (NSplx, n = 5) or a sham operation (n = 5) at 1 day after NTx and were analyzed at 8 weeks. (*D*) Four-week-old mice underwent a splenectomy (Splx, n = 5) or a sham operation (n = 5) and were analyzed at 8 weeks. (*E* and *F*) Twelve-week-old mice underwent a splenectomy (Splx, n = 5) or a sham operation (n = 5) and were analyzed at 20 weeks. (*B–E*) Liver staining with H&E and (*A* and *F*) serum levels of AST and ALT. *Bars* indicate the mean of each group, and the *error bars* indicate SD. *$P < .05$. *Scale bars* = 100 μm.

8-week-old C57BL/6-NTx-*PD-1*$^{-/-}$ mice (Figure 7*D* and Supplementary Figure 10*C* and *D*). Notably, splenectomy neither induced fatal infection nor decreased the survival rate (Supplementary Table 2), whereas splenectomy at 12 weeks suppressed AIH, sustaining remission until 20 weeks of age (Figure 7*E* and *F*). Thus, these data suggest that splenectomy has therapeutic efficacy for chronic AIH similar to fulminant AIH.

Discussion

Using the AIH models, we here examined the effects of treatment with DEX to find clues to overcoming therapeutic insufficiency of corticosteroids for AIH. We showed that T_{FH} cells in the spleen are responsible not only for the development of AIH but also for relapse after discontinuing treatment with corticosteroids. In BALB/

c-NTx-*PD-1*$^{-/-}$ mice, the spleen is the induction site for fatal AIH, and responsible T_{FH} cells are dysregulated in the spleen under the concurrent loss of Tregs and PD-1-mediated signaling. CCR6-CCL20 axis-dependent migration of these T cells triggers AIH.[12] In addition, fatal progression is mediated by further differentiation of Th1-type effector T cells from T_{FH} cells in the spleen, and a specific chemokine-dependent migration of those T cells is crucial for fatal progression (unpublished data, May 2013). We showed that injections of DEX are therapeutic for fatal AIH in this model whereas T_{FH} cells still exist in the spleen even after continuous administration of DEX; discontinuing treatment resulted in fatal AIH. In addition, residual splenic $CD4^+$ T cells were more resistant to DEX-mediated apoptosis after therapeutic injections of DEX, and transfer of these residual splenic $CD4^+$ cells induced the development of hepatitis in the recipient *RAG2*$^{-/-}$ mice. From these data, we concluded that in the mouse model of AIH, corticosteroid therapy has the drawback of allowing dysregulated T_{FH} cells to remain in the spleen.

We described another AIH model in which C57BL/6-NTx-*PD-1*$^{-/-}$ mice developed chronic hepatitis with fibrosis, hypergammaglobulinemia, and the production of ANA. Notably, dysregulated T_{FH} cells were generated in the spleen, neonatal splenectomy suppressed chronic AIH, and transfer of splenic $CD4^+$ T cells induced hepatitis in the recipient *RAG2*$^{-/-}$ mice. These results indicate that the same induction mechanisms are involved in the development of AIH in mice, with manifestations ranging from acute onset to chronic. In humans, it is unknown at present whether the spleen is the induction site of AIH or whether T_{FH} cells are responsible for the development of AIH, although splenomegaly is a common clinical finding in patients with active AIH.[1-3] Therefore, it is important to know whether similar mechanisms are involved in the relapse of AIH in humans after withdrawal of corticosteroids.

In our previous and present studies, we showed that splenectomy, either neonatal or at 7 or 10 days of age before the induction of AIH, suppressed AIH presenting as fulminant hepatic failure in BALB/c-NTx-*PD-1*$^{-/-}$ mice.[12] In this study, we revealed that neonatal splenectomy also suppressed the development of chronic AIH in C57BL/6-NTx-*PD-1*$^{-/-}$ mice. Because patients with severe AIH have a high potential for recurrence after liver transplantation, leading to a greater probability of graft loss, splenectomy might well prevent such recurrence.

Interestingly, we further observed in this study that splenectomy after the development of AIH suppressed liver inflammation with manifestations ranging from acute onset to chronic. In the acute AIH model, splenectomy alone suppressed liver inflammation and sustained remission for 4 weeks. In addition, splenectomy after treatment with DEX suppressed AIH and extended remission beyond 4 weeks. Moreover, in the chronic AIH model, splenectomy at 12 weeks of age suppressed AIH, sustaining remission until 20 weeks. It is well known that patients with AIH in remission after withdrawal of corticosteroid therapy are likely to experience a relapse and that multiple relapses are associated with poor prognosis.[7,8] Therefore, it is of interest to determine whether splenectomy might be considered in some patients with AIH, although this will need to be very carefully assessed given the concerns related to splenectomy.

In conclusion, we showed that although corticosteroid therapy has therapeutic efficacy for AIH in mice, it allows residual splenic dysregulated T_{FH} cells to remain after treatment, which appear to be responsible for relapse. In addition, we found that splenectomy overcomes this insufficiency, inducing prolonged remission of AIH. These data may prove useful in obtaining complete remission in humans with AIH.

Supplementary Material

Note: To access the supplementary material accompanying this article, visit the online version of *Gastroenterology* at www.gastrojournal.org, and at http://dx.doi.org/10.1053/j.gastro.2013.03.011

References

1. Krawitt EL. Autoimmune hepatitis. N Engl J Med 2006;354:54-66.
2. Manns MP, Czaja AJ, Gorham JD, et al. Diagnosis and management of autoimmune hepatitis. Hepatology 2010;51:2193-2213.
3. Czaja AJ, Manns MP. Advances in the diagnosis, pathogenesis, and management of autoimmune hepatitis. Gastroenterology 2010; 139:58-72.
4. Manns MP. Autoimmune hepatitis: the dilemma of rare diseases. Gastroenterology 2011;140:1874-1876.
5. Czaja AJ, Davis GL, Ludwig J, et al. Complete resolution of inflammatory activity following corticosteroid treatment of HBsAg-negative chronic active hepatitis. Hepatology 1984;4:622-627.
6. Czaja AJ. Safety issues in the management of autoimmune hepatitis. Expert Opin Drug Saf 2008;7:319-333.
7. Czaja AJ, Ammon HV, Summerskill WH. Clinical features and prognosis of severe chronic active liver disease (CALD) after corticosteroid-induced remission. Gastroenterology 1980;78:518-523.
8. Montano-Loza AJ, Carpenter HA, Czaja AJ. Consequences of treatment withdrawal in type 1 autoimmune hepatitis. Liver Int 2007; 27:507-515.
9. Montano-Loza AJ, Carpenter HA, Czaja AJ. Improving the end point of corticosteroid therapy in type 1 autoimmune hepatitis to reduce the frequency of relapse. Am J Gastroenterol 2007;102:1005-1012.
10. Hoeroldt B, McFarlane E, Dube A, et al. Long-term outcomes of patients with autoimmune hepatitis managed at a nontransplant center. Gastroenterology 2011;140:1980-1989.
11. Kido M, Watanabe N, Okazaki T, et al. Fatal autoimmune hepatitis induced by concurrent loss of naturally arising regulatory T cells and PD-1-mediated signaling. Gastroenterology 2008;135:1333-1343.
12. Aoki N, Kido M, Iwamoto S, et al. Dysregulated generation of follicular helper T cells in the spleen triggers fatal autoimmune hepatitis in mice. Gastroenterology 2011;140:1322-1333.
13. King C. New insights into the differentiation and function of T follicular helper cells. Nat Rev Immunol 2009;9:757-766.
14. Knodell RG, Ishak KG, Black WC, et al. Formulation and application of a numerical scoring system for assessing histological activity in asymptomatic chronic active hepatitis. Hepatology 1981;1:431-435.
15. Wyllie AH. Glucocorticoid-induced thymocyte apoptosis is associated with endogenous endonuclease activation. Nature 1980;284: 555-556.
16. Compton MM, Cidlowski JA. Rapid *in vivo* effects of glucocorticoids on the integrity of rat lymphocyte genomic deoxyribonucleic acid. Endocrinology 1986;118:38-45.

17. Chen X, Murakami T, Oppenheim JJ, et al. Differential response of murine CD4+CD25+ and CD4+CD25- T cells to dexamethasone-induced cell death. Eur J Immunol 2004;34:859-869.
18. Czaja AJ, Carpenter HA, Santrach PJ, et al. Significance of HLA DR4 in type 1 autoimmune hepatitis. Gastroenterology 1993; 105:1502-1507.
19. Czaja AJ, Strettell MD, Thomson LJ, et al. Associations between alleles of the major histocompatibility complex and type 1 autoimmune hepatitis. Hepatology 1997;25:317-323.
20. Nishimura H, Minato N, Nakano T, et al. Immunological studies on PD-1 deficient mice: implication of PD-1 as a negative regulator for B cell responses. Int Immunol 1998;10:1563-1572.
21. Schwabe RF, Brenner DA. Mechanisms of liver injury. I. TNF-α-induced liver injury: role of IKK, JNK, and ROS pathways. Am J Physiol Gastrointest Liver Physiol 2006;290:G583-G589.
22. Oksenberg JR, Stuart S, Begovich AB, et al. Limited heterogeneity of rearranged T-cell receptor Vα transcripts in brains of multiple sclerosis patients. Nature 1990;345:344-346.
23. Kim G, Tanuma N, Kojima T, et al. CDR3 size spectratyping and sequencing of spectratype-derived TCR of spinal cord T cells in autoimmune encephalomyelitis. J Immunol 1998;160:509-513.
24. Striebich CC, Falta MT, Wang Y, et al. Selective accumulation of related CD4+ T cell clones in the synovial fluid of patients with rheumatoid arthritis. J Immunol 1998;161:4428-4436.
25. Kato T, Kurokawa M, Masuko-Hongo K, et al. T cell clonality in synovial fluid of a patient with rheumatoid arthritis: persistent but fluctuant oligoclonal T cell expansions. J Immunol 1997; 159:5143-5149.
26. Sekine T, Kato T, Masuko-Hongo K, et al. Type II collagen is a target antigen of clonally expanded T cells in the synovium of patients with rheumatoid arthritis. Ann Rheum Dis 1999;58:446-450.
27. Tanaka A, Iwabuchi S, Takatori M, et al. Clonotypic analysis of T cells in patients with autoimmune and viral hepatitis. Hepatology 1997; 25:1070-1076.
28. Löhr HF, Pingel S, Weyer S, et al. Individual and common antigen-recognition sites of liver-derived T cells in patients with autoimmune hepatitis. Scand J Immunol 2003;57:384-390.
29. Arenz M, Pingel S, Schirmacher P, et al. T cell receptor Vβ chain restriction and preferred CDR3 motifs of liver-kidney microsomal antigen (LKM-1)-reactive T cells from autoimmune hepatitis patients. Liver 2001;21:18-25.
30. Dieckmann D, Plottner H, Berchtold S, et al. Ex vivo isolation and characterization of CD4(+)CD25(+) T cells with regulatory properties from human blood. J Exp Med 2001;193:1303-1310.
31. Baecher-Allan C, Brown JA, Freeman GJ, et al. CD4+CD25 high regulatory cells in human peripheral blood. J Immunol 2001; 167:1245-1253.
32. Liu W, Putnam AL, Xu-Yu Z, et al. CD127 expression inversely correlates with FoxP3 and suppressive function of human CD4+ T reg cells. J Exp Med 2006;203:1701-1711.

Received April 9, 2012. Accepted March 8, 2013.

Reprint requests

Address requests for reprints to: Norihiko Watanabe, Center for Innovation in Immunoregulative Technology and Therapeutics and Department of Gastroenterology and Hepatology, Graduate School of Medicine, Kyoto University, Kyoto 606-8501, Japan. e-mail: norihiko@kuhp.kyoto-u.ac.jp; fax: (81) 75-751-4303.

Acknowledgments

The authors thank Dr Taku Okazaki and Tasuku Honjo for providing PD-1-deficient mice; Dr Dovie Wylie for assistance in preparation of the manuscript; Ms Chigusa Tanaka for excellent technical assistance; and Drs Shuh Narumiya, Nagahiro Minato, Shimon Sakaguchi, Takeshi Watanabe, and Ichiro Aramori for critical discussion and suggestions.

Conflicts of interest

The authors disclose no conflicts.

Funding

The Center for Innovation in Immunoregulative Technology and Therapeutics is supported in part by the Special Coordination Funds for Promoting Science and Technology of the Japanese Government and in part by Astellas Pharma Inc in the Formation of Innovation Center for Fusion of Advanced Technologies Program. This work is partially supported by Grants-in-aid for Scientific Research 21229009 and 23590973 from the Japan Society for the Promotion of Science, a Health and Labour Sciences Research Grant for Research on Intractable Diseases, and Research on Hepatitis from the Ministry of Health, Labour and Welfare, Japan, Grants-in-Aid for Research by The Kato Memorial Trust for Nambyo Research, and The Waksman Foundation of Japan.

Supplementary Materials and Methods

Mice

C57BL/6 and BALB/c mice were purchased from Japan SLC (Shizuoka, Japan), and *PD-1*$^{-/-}$ and *RAG-2*$^{-/-}$ mice on a C57BL/6 or BALB/c background were generated as described.[1-3] All of these mice were bred and housed under specific pathogen-free conditions. Thymectomy and splenectomy of the mice were performed as described.[4-6] The sham splenectomy was performed by cutting the peritoneum without removing the spleen. All mouse protocols were approved by the Institute of Laboratory Animals, Graduate School of Medicine, Kyoto University.

Administration of DEX In Vivo

For the preventive protocol, starting 1 day after thymectomy, BALB/c-NTx-*PD-1*$^{-/-}$ mice were intraperitoneally injected every other day with 1.0 mg/kg DEX (Sigma-Aldrich, St Louis, MO) diluted in PBS or PBS alone. After 13 injections, mice at 4 weeks of age were killed, and the livers, spleens, and sera were harvested. For the therapeutic protocol, starting 14 days after thymectomy, BALB/c-NTx-*PD-1*$^{-/-}$ mice were intraperitoneally injected every other day with 1.0 mg/kg DEX diluted in PBS or PBS alone. In C57BL/6-NTx-*PD-1*$^{-/-}$ mice, therapeutic injections of 0.5 mg/kg DEX every other day were started at 4 weeks of age. After the indicated injections, the mice were killed.

Histological and Immunohistological Analysis

Organs were fixed in neutral buffered formalin and embedded in paraffin wax. Sections were stained with H&E or Masson's trichrome for histopathology. Fluorescence immunohistology was performed on frozen sections as described previously[4,5] using fluorescein isothiocyanate (FITC)-conjugated anti-CD4 (RM4-5), anti-CD8a (Ly-2) (eBioscience, San Diego, CA), peanut agglutinin (PNA; Vector Laboratories, Burlingame, CA), and biotin-labeled anti-B220 (RA3-6B2; BD Biosciences, San Jose, CA) followed by Texas Red–conjugated avidin (Vector Laboratories). To detect autoantibodies, livers were collected from wild-type BALB/c and C57BL/6 mice. Sections were stained with 100× to 3200× diluted sera from indicated mice, followed by FITC-conjugated anti-mouse IgG (Cappel, Chester, PA).[4]

Flow Cytometry Analysis and Isolation of Lymphocytes

Single cells from the livers and spleens were prepared as described.[4,5] The following monoclonal antibodies were used for surface staining: FITC-conjugated anti-CD4, anti-CXCR5 (2G8), anti-GL7, anti-CD11c (*HL3*) (BD Biosciences), and anti-DX5 (eBioscience); PE-conjugated anti-CD3e (145-2C11), anti-ICOS, and anti–Gr-1 (RB6-8C5) (eBioscience); anti-CD95/Fas (Jo2) (BD Biosciences); APC-Cy7–conjugated anti-CD4 (GK1.5) and biotin-labeled B220 (BD Biosciences); and APC-conjugated streptavidin, anti-CD8a, anti-CD25 (PC61.5), and anti-CD11b (M1/70) (eBioscience). For flow cytometric analysis of splenic $CD4^+$ T cells in Figure 2*C* and Supplementary Figure 6*A*, spleen cells were stained with FITC/anti-CXCR5, PE/anti-ICOS, and APC-Cy7/anti-CD4. To analyze splenic $B220^+$ B cells in Figure 4*B*, cells were stained with FITC/anti-GL7, PE/anti-CD95/Fas, and biotin-labeled B220 followed by APC-conjugated streptavidin. Data of flow cytometric analysis in Figure 5*E* and *F* represent cell numbers of the following cell subsets in the liver: $CD11b^+CD11c^-$ macrophages, $CD11c^+$ dendritic cells, $CD11b^+Gr\text{-}1^+$ myeloid cells, $CD3^-DX5^+$ natural killer cells, $CD3^+DX5^+$ natural killer T cells, $CD3^+DX5^-$ T cells, $B220^+$ B cells, $CD3^+CD4^+$ T cells, and $CD3^+CD8^+$ T cells. For the analysis of TCR V_β use in Figure 6*F*, cells were stained with FITC/anti-V_β2 (B20.6), anti-V_β3 (KJ25), anti-V_β4 (KT4), anti-V_β5.1 and V_β5.2 (MR9-4), anti-V_β6 (RR4-7), anti-V_β7 (TR310), anti-V_β8.1 and V_β8.2 (MR5-2), anti-V_β8.3 (IB3.3), anti-V_β9 (MR10-2), anti-$V_\beta10^b$ (B21.5), anti-V_β11 (RR3-5), anti-V_β12 (MR11-1), anti-V_β13 (MR12-3), anti-V_β14 (14-2), anti-$V_\beta17^a$ (KJ23), PE/anti-CD3e, and APC-Cy7/anti-CD4 for $CD4^+$ T cells using the Mouse V_β TCR Screening Panel (BD Biosciences). Stained cells were analyzed with a FACSCanto II (BD Biosciences). Data were analyzed using CellQuest Pro (BD Biosciences). Dead cells were excluded on the basis of side- and forward-scatter characteristics, and viable cell numbers were calculated as follows: (Percentage of Cells in the Cell Type) × (Number of Viable Cells). For 7-AAD staining in Figure 2*D*, single cells were isolated from the spleens of 3-week-old BALB/c-NTx-*PD-1*$^{-/-}$ mice injected with DEX therapeutically. Isolated spleen cells (1×10^6) were cultured with 10–1000 ng/mL DEX under plate-bound anti-CD3 (1 μg/mL) and soluble anti-CD28 (5 μg/mL). Round-bottomed 96-well culture plates were used with Dulbecco's modified Eagle medium supplemented with 10% fetal bovine serum, 50 mmol/L 2-mercaptoethanol, 100 U/mL penicillin, and 100 μg/mL streptomycin. Three days after the culture, cells were harvested and stained with FITC-conjugated anti-CD3e (eBioscience) and 7-AAD (BD Biosciences) and either PE/Texas Red–conjugated anti-CD4 (Abcam, Cambridge, England) or PE/Texas Red–conjugated anti-CD8 (Abcam). In Foxp3 staining, cells were fixed and permeabilized using Foxp3 staining buffer (eBioscience) and stained with PE/anti-Foxp3 (eBioscience).

ELISA

Serum Ig levels were determined by ELISA as described,[7] and antibody sets to detect mouse IgG1, IgG2a, IgG2b, and IgG3 (BD Biosciences) and anti-mouse IgM (AbD Serotec, Oxford, England) were used. To detect serum ANAs, microtiter plates (Nunc, Roskilde, Denmark) were incubated with 10 μg/mL antigen, and the nuclear fraction was prepared from normal liver.[8] Antibody sets to detect mouse ANA subclasses were the same as previously described. Serum concentrations of TNF-α and interferon gamma were measured with mouse cytokine ELISA sets (eBioscience) according to the manufacturer's protocols.

Isolation of Lymphocytes and Adoptive Transfer

For transfer of total spleen cells, BALB/c-NTx-*PD-1*$^{-/-}$ mice at 14 days after thymectomy were intraperitoneally injected every other day with or without 1.0 mg/kg DEX diluted in PBS. Single cells were isolated from the spleens of 3-week-old mice. Isolated spleen cells (1×10^7) were intravenously injected into *RAG2*$^{-/-}$ recipient mice on a BALB/c background at 4 to 6 weeks of age. To transfer CD4$^+$ T cells or CD4$^+$ T cell-depleted spleen cells, 3-week-old BALB/c-NTx-*PD-1*$^{-/-}$ mice were therapeutically injected with DEX. Cells were prepared using mouse CD4 microbeads (Miltenyi Biotec, Bergisch Gladbach, Germany) according to the manufacturer's protocols. Purity was assessed by flow cytometry. CD4$^+$ T cells were purified to reach >90% purity, and CD4$^-$ splenocytes reached >99% purity. Isolated cells (1×10^6) were intravenously injected into BALB/c-*RAG2*$^{-/-}$ mice at 4–6 weeks of age.

For transfer of CD4$^+$ T cells from C57BL/6-*PD-1*$^{-/-}$ mice, CD3$^+$CD4$^+$ T cells were prepared from the spleens of 8-week-old C57BL/6-*PD-1*$^{-/-}$ mice with or without NTx obtained using a FACSAria II. Isolated CD3$^+$CD4$^+$ T cells (1×10^6) were intravenously injected into C57BL/6-*RAG2*$^{-/-}$ recipient mice at 4 to 6 weeks of age. For transfer, CD4$^+$CD25$^+$ Tregs were purified from the spleens of 8-week-old C57BL/6-*PD-1*$^{-/-}$ mice. Tregs were obtained using a FACSAria II and isolated with a CD4$^+$CD25$^+$ T cell to reach >99% purity. Tregs (1×10^6) were intravenously injected into C57BL/6-NTx-*PD-1*$^{-/-}$ mice at 4 weeks of age. Four weeks after transfer, the recipient mice at 8 weeks of age were killed.

HAI Score

Histological activity of chronic active hepatitis was assessed according to a semiquantitative scoring system, as described previously for humans.[9] For histological assessment, all specimens were reviewed in a blinded manner by at least 2 hepatologists. Using Knodell's HAI scoring system, liver specimens were graded in 4 categories. Category I, periportal and/or bridging hepatocellular necrosis, was graded from 0 to 10, where 0 = none, 1 = mild piecemeal necrosis, 3 = moderate piecemeal necrosis (involves less than 50% of the circumference of most portal tracts), 4 = marked piecemeal necrosis (involves more than 50% of the circumference of most portal tracts), 5 = moderate piecemeal necrosis plus bridging necrosis, 6 = marked piecemeal necrosis plus bridging necrosis, and 10 = multilobular necrosis. Category II, intralobular degeneration and focal hepatocellular necrosis, was graded from 0 to 4, where 0 = none, 1 = mild (acidophilic bodies, ballooning degeneration, and/or scattered foci of hepatocellular necrosis in less than one-third of lobules or nodules), 3 = moderate (involvement of one-third to two-thirds of lobules or nodules), and 4 = marked (involvement of more than two-thirds of lobules or nodules). Category III, portal inflammation, was graded from 0 to 4, where 0 = no portal inflammation, 1 = mild (sprinkling of inflammatory cells in less than one-third of portal tracts), 3 = moderate (increased inflammatory cells in one-third to two-thirds of portal tracts), and 4 = marked (dense packing of inflammatory cells in more than two-thirds of portal tracts). Category IV, fibrosis, was graded from 0 to 4, where 0 = no fibrosis, 1 = fibrous portal expansion, 3 = bridging fibrosis (portal-portal or portal-central linkage), and 4 = cirrhosis.

Supplementary References

1. Nishimura H, Minato N, Nakano T, et al. Immunological studies on PD-1 deficient mice: implication of PD-1 as a negative regulator for B cell responses. Int Immunol 1998;10:1563–1572.
2. Nishimura H, Okazaki T, Tanaka Y, et al. Autoimmune dilated cardiomyopathy in PD-1 receptor-deficient mice. Science 2001; 291:319–322.
3. Shinkai Y, Rathbun G, Lam KP, et al. RAG-2-deficient mice lack mature lymphocytes owing to inability to initiate V(D)J rearrangement. Cell 1992;68:855–867.
4. Kido M, Watanabe N, Okazaki T, et al. Fatal autoimmune hepatitis induced by concurrent loss of naturally arising regulatory T cells and PD-1-mediated signaling. Gastroenterology 2008;135: 1333–1343.
5. Aoki N, Kido M, Iwamoto S, et al. Dysregulated generation of follicular helper T cells in the spleen triggers fatal autoimmune hepatitis in mice. Gastroenterology 2011;140:1322–1333.
6. Klonowski KD, Marzo AL, Williams KJ, et al. CD8 T cell recall responses are regulated by the tissue tropism of the memory cell and pathogen. J Immunol 2006;177:6738–6746.
7. Muramatsu M, Kinoshita K, Fagarasan S, et al. Class switch recombination and hypermutation require activation-induced cytidine deaminase (AID), a potential RNA editing enzyme. Cell 2000; 102:553–563.
8. Blobel G, Potter VR. Nuclei from rat liver: isolation method that combines purity with high yield. Science 1966;154:1662–1665.
9. Knodell RG, Ishak KG, Black WC, et al. Formulation and application of a numerical scoring system for assessing histological activity in asymptomatic chronic active hepatitis. Hepatology 1981; 1:431–435.

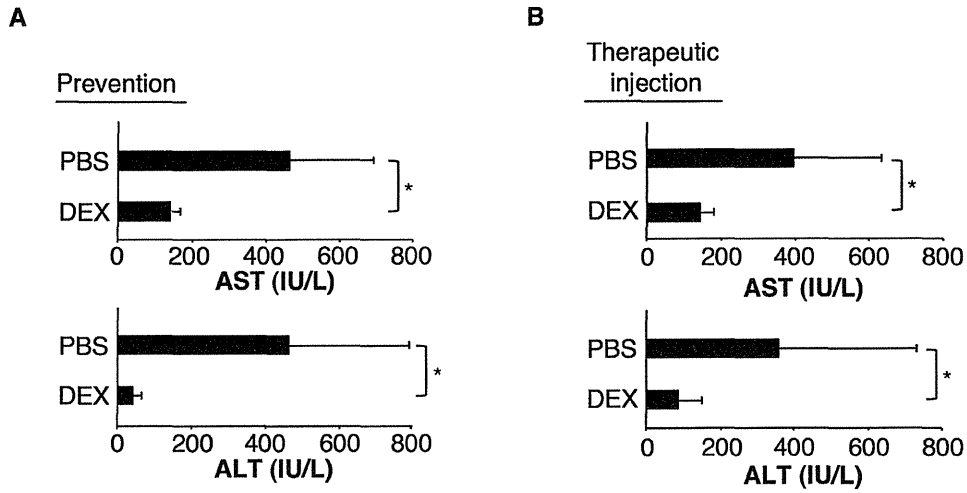

Supplementary Figure 1. Either preventive or therapeutic injection of DEX suppresses fatal AIH in BALB/c-NTx-*PD-1*$^{-/-}$ mice. (*A*) Starting 1 day after thymectomy, BALB/c-NTx-*PD-1*$^{-/-}$ mice were intraperitoneally injected every other day with 1.0 mg/kg DEX diluted in PBS (n = 5) or PBS alone (n = 17). After 13 injections, mice at 4 weeks of age were killed and sera were harvested. Serum levels of the liver transaminases AST and ALT are shown. (*B*) Starting 14 days after thymectomy, NTx-*PD-1*$^{-/-}$ mice were intraperitoneally injected every other day with 1.0 mg/kg DEX diluted in PBS (n = 11) or PBS alone (n = 13). After 6 injections, mice at 4 weeks of age were killed. Serum levels of AST and ALT are shown. *Bars* indicate the mean of each group, and the *error bars* indicate SD. *$P < .05$.

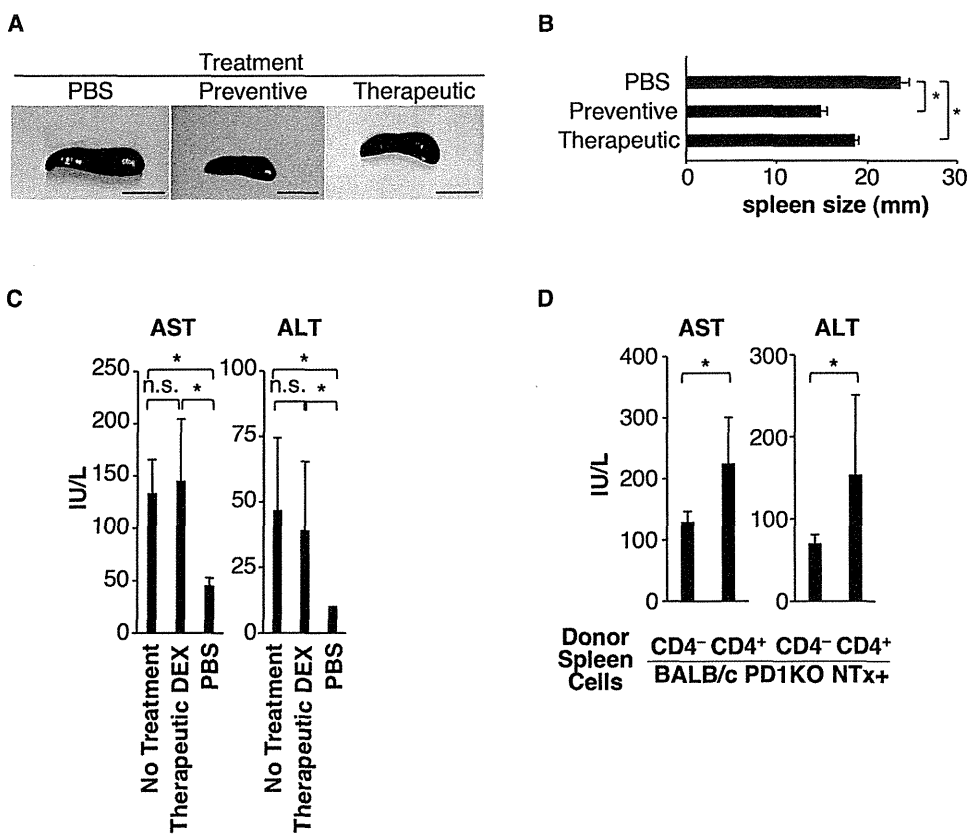

Supplementary Figure 2. Therapeutic administration of DEX reduces the size of the spleen, and residual CD4$^+$ T cells in the spleen of BALB/c-NTx-*PD-1*$^{-/-}$ mice can induce hepatitis. BALB/c-NTx-*PD-1*$^{-/-}$ mice were injected with DEX or PBS alone preventively or therapeutically, as described in Figure 1. (*A*) Macroscopic view of spleen. (*B*) Splenic sizes. (*C* and *D*) Serum levels of the liver transaminases AST and ALT in recipient BALB/c-*RAG2*$^{-/-}$ mice 3 weeks after transfer. Total splenocytes were solated and transferred from BALB/c-NTx-*PD-1*$^{-/-}$ mice with or without therapeutic injections of DEX (*C*). Purified splenic CD4$^+$ T cells or CD4$^+$ T cell–depleted splenocytes (CD4$^-$ cells) were transferred from BALB/c-NTx-*PD-1*$^{-/-}$ mice therapeutically treated with DEX (*D*). *Bars* indicate the mean of each group, and the *error bars* indicate SD. *$P < .05$. n.s., not significant. *Scale bars* = 1 cm.